ABSTRACT

Designing Quantitative Structure Activity Relationships (QSAR) to Predict Specific Toxic Endpoints for Polybrominated Diphenyl Ethers (PBDE) in Mammalian Cell Culture Systems

Swati Rawat, M.S.

Advisor: Erica D. Bruce, Ph.D.

Polybrominated diphenyl ethers (PBDEs) are becoming increasingly known as effective flame retardants and have vast industrial application in products like plastics, building materials, and textiles. They are found to be structurally similar to thyroid hormones that are responsible for regulating metabolism in the body. Structural similarity with the hormones poses a threat to human health because once in the system, the PBDEs may change thyroid hormone transport and metabolism. This study is aimed at designing QSAR models for predicting toxic endpoints for PBDEs in mammalian cells. QSAR modeling uses the known chemicals' activity, which serve as surrogates to study unknown chemicals belonging to the same family. This research is a threefold process including running in-vitro bioassays to collect data on the toxic endpoints, modeling the evaluated endpoints using QSARs and validating the models using compounds of interest from the same family (PBDEs).

Designing Quantitative Structure Activity Relationships (QSAR)
to Predict Specific Toxic Endpoints for Polybrominated Diphenyl Ethers (PBDE)
in Mammalian Cell Culture Systems

by

Swati Rawat, B.Tech.

A Thesis

Approved by the Department of Environmental Science

_____
George P. Cobb, Ph.D., Chairperson

Submitted to the Graduate Faculty of
Baylor University in Partial Fulfillment of the
Requirements for the Degree
of
Master of Science

Approved by the Thesis Committee

_____
Erica D. Bruce, Ph.D., Chairperson

_____
Bryan W. Brooks, Ph.D.

_____
Mary Lynn Trawick, Ph.D.

Accepted by the Graduate School
December 2011

_____
J. Larry Lyon, Ph.D., Dean

Page bearing signatures is kept on file in the Graduate School.

Copyright © 2011 by Swati Rawat

All rights reserved

TABLE OF CONTENTS

List of Figures v
List of Tables vii
List of Abbreviations viii
Acknowledgments x

Chapter One - Introduction

Introduction 1
Literature Review 4
Significance 10
Specific Objectives and Hypothesis 13

Chapter Two - Methods

Cell Culture and Bioassays for Specific Endpoints 15
Analytical Verification of Chemical Stock Solutions 16
Determination of Cell Viability by Janus Green B 17
Determination of Oxidative Stress by DCFH-DA 18
Determination of Apoptosis by Caspase Assay 19
Statistical Methods 22
Building QSAR in Discovery Studio (Accelyrs Inc, San Diego, CA) 22

Chapter Three - Results

Results from Analysis of Chemical Stock Solutions 27
Toxicity Metric 27

Chapter Four - Discussion and Conclusions

Discussion 50
Control Variability 51
Cell Viability 52
Oxidative Stress 59
Apoptosis 62
Conclusions 67

References

Appendix 70
Bibliography 84

LIST OF FIGURES

Figure 1. Structure of polybrominated diphenyl ethers.....1

Figure 2. Structure of Janus Green.....18

Figure 3. Mechanism of action of DCFH-DA. Adapted from Invitrogen® (Carlsbad, CA, USA) Molecular Probes handbook, product number D688319

Figure 4. Bisamide derivative of Rhodamine 110 (Z-DEVD-R110, the substrate). Adapted from Invitrogen® (Carlsbad, CA, USA) Molecular Probes handbook, product number E13184.....21

Figure 5. Mechanism of action of caspase-3 protease on Z-DEVD-R110 to highly fluorescent R110 in two steps. Adapted from Invitrogen® (Carlsbad, CA, USA) Molecular Probes handbook, product number E13184.....22

Figure 6. Percentage viability of Hep G2 cells exposed to different nominal concentrations of PBDE parent congeners.....29

Figure 7. Percentage viability of Hep G2 cells exposed to different nominal concentrations of PBDEs hydroxylated congeners.....30

Figure 8. Percentage viability of Hep G2 cells exposed to varying nominal concentrations of PBDE congeners to be used as test chemicals.....31

Figure 9. QSAR for cell viability responses elicited by the training set chemicals. Predicted log toxicity versus experimental log toxicity.....32

Figure 10 Validation run for cell viability QSAR. Predicted log toxicity versus experimental log toxicity.....32

Figure 11. Percentage oxidative stress in Hep G2 cells exposed to different nominal concentrations of parent PBDE congeners.....34

Figure 12. Percentage oxidative stress in Hep G2 cells exposed to different nominal concentrations of hydroxylated PBDE congeners.....35

Figure 13. Percentage oxidative stress in Hep G2 cells exposed to different nominal concentrations of PBDE congeners (test chemicals).....36

Figure 14. QSAR for oxidative stress responses elicited by the training set chemicals. Predicted log oxidative stress versus experimental log oxidative stress.....37

Figure 15. Validation run for oxidative stress QSAR. Predicted log oxidative stress versus experimental log oxidative stress 37

Figure 16. Percentage caspase-3 activity responses in Hep G2 cells exposed to different nominal concentrations of parent PBDE congeners.....38

Figure 17. Percentage caspase-3 activity responses in Hep G2 cells exposed to different nominal concentrations of hydroxylated PBDE congeners 40

Figure 18. Percentage caspase-3 activity responses in Hep G2 cells exposed to different nominal concentrations of PBDE congeners (test chemicals) 41

Figure 19. QSAR for the caspase-3 activity responses elicited by the training set chemicals. Predicted log apoptosis versus experimental log apoptosis 42

Figure 20. Validation run for caspase-3 activity QSAR. Predicted log apoptosis versus experimental log apoptosis 42

LIST OF TABLES

Table 1. Lowest observable adverse effect concentration (LOAEC) values from invitro experiments used for generating QSAR equations 44

Table 2. Relevant statistics for the developed QSARs 45

Table 3. Relevant ANOVA statistics for cell viability studies 47

Table 4 Relevant ANOVA statistics for oxidative stress studies.....48

Table 5 Relevant ANOVA statistics for apoptosis studies 49

Table 6 Log K_{ow} values for specific PBDE congeners.....61

LIST OF ABREVIATIONS

AD- Applicability domain

ANOVA- Analysis of Variance

AR- Androgen receptor

BFRs- Brominated Flame Retardants

CMP- Calculate Molecular Properties

DCF- Dichlorofluorescein

DCFH-DA- Dicholofluorescene diacetate

DMSO- Dimethyl sulfoxide

DR- Dioxin receptor

DS- Discovery Studio

EC- Effective concentration

ER- Estrogen receptor

EROD- Ethoxyresorufin O-deethylase assay

E-state- Electrotopological state

FIRE- Flame retardants Integrated Risk assessment for Endocrine effects

GFA- Genetic function approximation

GJIC- Gap junction intercellular communication assay

HBCD- hexabromocyclododecane

Hep G2- Human hepatocarcinoma

LOAEC- Lowest observable adverse effect concentration

LOF- Lack of fit

MR- Molar refractivity

NOAEC- No observable adverse effect concentration

OS- Oxidative Stress

PBDEs- Polybrominated Diphenyl Ethers

PR- Progesterone receptor

PRESS- Predicted residual sum of squares

QM- Quantum mechanical

QSARS- Quantitative Structure-Activity Relationship

QSTR- Quantitative Structure Toxicity Relationship

RMSE- Root mean square error

ROS- Reactive oxygen species

SEM– Standard error about the mean

SH-SY5Y- Human neuroblastoma

SMILES- Simplified Molecular Input Line Entry Specification

SOR- Significance of regression

TBBPA- Tetrabromobisphenol A

TEFs- Toxic equivalency factors

TIs- Topological indices

ACKNOWLEDGMENTS

I feel indebted to Baylor University for providing me with the opportunity of being able to pursue the degree and gain fruitful experience. I would like to extend my heartfelt gratitude to my advisor Dr. Erica D. Bruce, for her kind patience, constant support and careful guidance at every step of my research. Her easy approachability, constructive criticism, and persistent encouragement leveraged the research project. I would also like to thank the thesis committee members, Dr. Bryan W. Brooks, and Dr. Mary Lynn Trawick for their invaluable contributions towards this project.

Also, my lab mates Krystal Pree, Fan Zhang, Nick Saltarelli, Eleanor Robinson, Bikram Subedi, Lissette Aguilar and Krystal Usenko played an instrumental role in bringing this project together. My family has always provided me with motivation, love and inspiration that have been the foundation of my professional life, with no exception to this project. Words cannot fathom my gratitude and respect for them.

A special note of thanks to the Glasscock family for making available Glasscock Funds for Excellence in Environmental Sciences, without which the research would not have been possible.

Swati Rawat

CHAPTER ONE

Introduction

Polybrominated diphenyl ethers (PBDEs) are a class of organic compounds that have a wide industrial application as flame retardants. PBDEs have been used in a wide range of products like plastics, building materials, airplanes, electronics, upholstery, furnishings, polyurethane foams, motor vehicles, and textiles. The addition of PBDEs to the manufacturing process aims to make the products difficult to burn. They are structurally similar to PCBs (Figure 1).

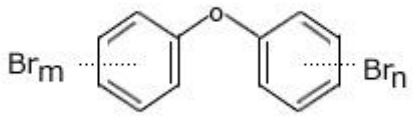

Figure 1. Structure of polybrominated diphenyl ethers (adapted from Wikipedia)

The family of PBDEs has 209 congeners (PBDE = C_{12} H_{10-x} Br_x O (x= 1, 2, 3,…….. 10 = m+n)). They are marketed under the trade names of DE-60F, DE-61, DE-62, and DE-71 in the US. The commercially available forms of PBDEs are not a single compound; rather they are mixtures of congeners.

PBDEs as flame retardants are not chemically (covalently) bonded to the polymer particles of the plastic, textile, or other raw material but are physically attached, at levels ranging from 5% to 30% (w/w). This allows PBDEs to leach out and spread to the surrounding dust particles of an indoor or occupational setting. The PBDE congeners have been reported to be observed in natural matrices like sand, sediment, and soil. They have been observed to bioaccumulate and

biomagnify in biota. There has been a ban on the production of PBDEs (PentaBDE and OctaBDE) in Europe and a voluntary discontinuation in some parts of the US. Nevertheless, the majority of the world's population is still prone to exposure. The main routes of exposure for humans include ingestion of contaminated foods (meat and dairy), inhalation, and ingestion and/or dermal uptake of house dust containing PBDEs released from electrical appliances and furniture (Meeker et al., 2009).

Structurally, the most active site in these chemicals is the bromine atom which is responsible for fire suppression. The bromine containing fire retarding compound produces hydrobromic acid that decelerates the chain combustion reaction of air in fire. The highly reactive hydrogen, oxygen, and hydroxy group react with hydrobromic acid and produce bromine radicals that are not very reactive. These react with the earliest radicals and help slow down the reaction towards termination. Although there are a wide variety of brominated flame retardants (BFRs), there are three major BFRs that are commercially produced on an industrial scale and used widely; tetrabromobisphenol A (TBBPA), hexabromocyclododecane (HBCD), and decarbrominated diphenyl ether (BDE 209). They accounted for an annual total market consumption of 223,482 metric tons in the year 2003. These compounds vary structurally, as do their lipophilicity, bioaccumulation, and environmental persistence, all of which are dependent on the number of bromine atoms. There has been a considerable amount of research on PBDEs and their effects in Europe, Japan, and North America. These studies show a high degree of bioavailability, bioaccumulation, and biomagnification of these compounds in aquatic systems. A study of marine species, especially predators at

the top of the food chain, show traces of lower brominated diphenyl ethers. There have been several time-related studies that show trends in biota and sediment. Most concerning are the observations made in human blood and mother's milk which, in general, show rising trends in PBDE levels during the past 30 years (Harju et al., 2007).

Experiments show that PBDEs or their metabolites may influence thyroid function by changing thyroid hormone transport and metabolism/deactivation. They may bind to thyroid hormones or other receptors and may cause a direct effect on thyroid gland tissues (Meeker et al., 2009). This is important because the receptor-ligand interaction with the xenobiotic may hamper the normal function of thyroid hormones which is to regulate metabolism of the body. Thyroid hormones indirectly influence cellular metabolism through their effect on most types of tissues. Hormones like thyroxin play a vital role in cell growth and differentiation. An adverse effect on the thyroid hormone homeostasis may result in every system of the body being affected; its function hampered may negatively influence the overall growth of the body (Talsness, 2008).

There is increasing application of quantitative structure activity relationships (QSAR) in toxicological research. Activity relationship models convey information about the structure and activity relationship of a compound. It is a representation of the biological and chemical effects of a compound as a function of its structure. QSARs evaluate how the structural, chemical, physical, and other properties of a compound relate to its biological activity. In large-scale scientific investigations, the method is used to estimate effects of chemicals when the

relevant test data for them are unavailable. Hydrophobicity, topology, electrical properties, carcinogenicity, estrogenecity, teratogencity, steric effects, and other descriptors, among the physicochemical properties that models are designed for, serve as the independent properties of the equation describing the modeled activity (Suter et al., 2007). One of the most common means of QSAR development is regression modeling. This necessitates one important property of the chemical that serves as the dependent property of the QSAR equation. A classic example of a Quantitative Structure Toxicity Relationship (QSTR) (equation 1) shows how the octanol/water partitioning coefficient, K_{ow}, of a chemical relates with its acute toxicity in a guppy. The acute toxicity is measured in terms of mean lethal concentration (LC_{50}).

$$\text{Log } (1/LC_{50}) = 0.871 \text{ (log } K_{ow}) - 4.87 \text{ (Koenemann, 1981)} \quad (1)$$

Literature Review

There has been increasing use of PBDEs on an industrial scale and along with that a rising awareness to investigate their adverse effects on human physiology. They pose a threat to human health due to their long half-life and characteristic thyroid hormone disrupting potency. Proliferation characteristics, apoptosis, oxidative stress, and cell viability are important for the class of PBDEs. They are also known for their bioaccumulation and bioconcentration potentials in the environment. Studies like the one by Gustafsson et al., (1999), illustrate the fact that bioconcentration factors for PBDEs -47, -99 and -153 in lab study with blue mussel lie in the range 220,000 to 1,400,000. Bioconcentration factor is an important indicator of toxicity. It is the ratio of the concentration of a particular

chemical in a tissue per concentration of chemical in the medium. It shows what concentration of any toxic substance is taken up by an organism from the surrounding medium. The substance would cause varying degrees of toxic effect only upon varying uptake. Traces of the chemicals have been found in fish from rivers in Illinois and Michigan and in peregrine falcons. There have been an alarmingly high number of reports about rising PBDE concentrations in human breast milk, bringing to light their lipophilicity. In one such study conducted in Sweden the concentration increased by a factor of 60 from 1972 to 1997. A maximum of about 419 ng PBDE congener/g of lipid was observed in Texas alone in a study conducted by Schecter et al., (2003), and a upper limit of 462 ng PBDE/g fat in sample of breast adipose tissue from San Francisco (Talsness et al., 2008). Hereafter, various studies conducted to evaluate the toxicity, fate, transport and mechanisms of PBDEs in the environment have been brought to notice.

Apoptosis, or programmed cell death, usually occurs in multicellular organisms. It is characterized by cell death and other morphological changes. Cell blebbing and shrinkage, fragmentation of chromosomal DNA and that of the nucleus, chromatin condensation are characteristics typical to apoptosis. He et al., (2008), used flow cytometry to study apoptosis induced in primary cultured rat hippocampal neurons following exposure to PBDE-47. They observed that when the cells were exposed to 41.2 μM PBDE-47 the percentage of apoptosis increased significantly (He et al., 2008). In another study conducted by Madia et al., (2004), human astrocytoma cells showed signs of apoptosis following exposure

to PBDE-99. Hence, the contribution of apoptosis in neurotoxic mechanisms of PBDE-99 was evident. An et al., (2010), studied the cytotoxic effects of 6-OH-BDE-47 and 6-MeO-BDE-47 in the year. They similarly used flow cytometry and found out that both of these metabolites of BDE-47 induce apoptosis in a dose dependent manner, 6-OH-BDE-47 relatively greater than 6-MeO-BDE-47 under the same experimental conditions.

Cell viability is the status of cells to survive, grow, and multiply. It is a measure of the number of cells that survive the toxic influence of a certain chemical at different concentrations. A study was designed to determine the anti-proliferative, apoptotic characteristics of PBDE-209 using human hepatocarcinoma (Hep G2) cells (Hu et al., 2007). Hep G2 cells were cultured and exposed to PBDE-209 at different concentrations (1.0-100.0 μmol/L) in a 72-hour study. The MTT assay was used as a tool to determine the cell viability and resulted in the observation that the chemical countered the cell viability in a time and concentration- dependent manner at concentrations ranging from 10.0-100.0 μmol/L. Effects such as the morphological changes, apoptosis, and cell cycle changes were examined and the anti-proliferative effect of PBDE-209 contributed to apoptosis in Hep G2 cells. Chen et al.,..(2009), experimented with neonatal rat hippocampal neurons to study the apoptotic rate, cell viability, calcium ion concentration, global gene DNA methylation levels, and oxidative stress on exposure to PBDE-209. The test outcomes clearly indicate that PBDE-209 decreases cell viability, increases the rate of apoptosis, and could cause oxidative stress. Similarly, PBDE-209 can reduce global gene DNA methylation levels and affect secondary messengers.

In a study with human neuroblastoma (SH-SY5Y) cells cultured in vitro, cells were grown with varying concentrations of PBDE-47 (1, 2, 4, 8 μg/l) in a 24 hr study (He et al., 2007).The outcomes indicated genotoxic and cytotoxic influences such as cell viability, apoptosis, DNA breakage, and cytogenetic damage, reactive oxygen species formation, lactate dehydrogenase leakage and cell proliferation under the PBDE-47 treatment.

Oxidative stress is caused by an imbalance in the reactive oxygen species production and their detoxification in any tissue system. Peroxides and free radicals that result from such an imbalance in redox state of the tissue cause toxicity in cell organelles like the DNA, proteins and lipids. Moderate oxidative stress may trigger apoptosis, severe stress due to oxidative species may cause cell death and very intense stress causes necrosis. The study by He et al., (2008), shows that PBDE 47 increases ROS formation. It shows that PBDE-47 exposure could result in oxidative stress in primary rat hippocampal neurons at levels low as substrates, enzymes, and products. He et al., (2008), that PBDE-47 may cause a concentration dependent rise in ROS production. When the cells were incubated with PBDE-47 at high concentrations (4-8 μg/ml), there was a decrease observed in SOD activity and glutathione levels while the MDA content was found to increase. In another study done by Reistad and Mariussen (2005), human granulocytes were exposed to BDE-71 and BDE-47 in vitro. They were found to increase ROS formation varying in a concentration-dependent manner. Fernie et al., (2005), observed that exposure to PBDEs induced oxidative stress with

increased oxidized glutathione, increased hepatic GSSG:GSH ratio and a slight increase in lipid per oxidation.

QSAR modeling has various advantages over the traditional method of scientific experimentation. It is an efficient, economical, time sensitive, and statistically robust method of determining toxicity of chemicals. QSAR modeling has become all the more valuable in times of depleting resources for scientific studies (Bruce et al., 2008) given the economic downturn. In addition, there are limited experimental data available that can enable toxicological and environmental profiling of emerging environmental contaminants, more specifically for the endocrine disrupting chemicals like brominated flame retardants (Papa et al., 2010). In such a scenario, *in silico* or computational tools like QSARs play a vital role in the process of risk assessment (Jacobs, 2004).

Genetic function approximation (GFA) technique is used for QSAR modeling in the present work. This is a relatively new method as compared to the more conventional methods for QSAR and QSTR modeling like correlation and regression analysis. The GFA method is an analogy of DNA evolution upon several rounds of generations in which an individual bit of strings is treated as a gene. The method has number of advantages over other popular methods. For example it gives more than one equation as output. It provides not only linear polynomials but also higher order polynomials, splines and Gaussians that enable automatic outlier removal. It offers immense statistical information not possible with other methods (Rogers and Hopfinger, 1993).

In the study conducted by Harju et al., (2006), to develop QSARs to aid human and environmental risk assessment processes for brominated flame retardants (BFRs), the data were generated by the in vitro screening program of FIRE (Flame retardants Integrated Risk assessment for Endocrine effects). QSARs were designed to analyze the potential of BFRs for damaging the endocrine system and to identify critical structural elements and physicochemical properties of the BFRs in relation to their endocrine disrupting potency (Harju et al., 2006). The findings consist of data sets of the potencies of BFRs to interact as agonists or antagonists with the androgen receptor (AR), progesterone receptor (PR), estrogen receptor (ER) and dioxin receptor (DR). All BFRs were tested for their potency to inhibit estradiol (E_2) sulfation by E_2 – sulfotransferase (E_2SULT) along with their potencies for displacing T_4 from TTR (Harju et al., 2006).

Bruce et al., (2008), used QSAR modeling to predict toxic endpoints for polyaromatic hydrocarbons (PAHs). This study used QSARs to develop models to predict endpoints in three bioassays that related to the particular stages of carcinogenesis (activation, initiation, promotion and progression). The ethoxyresorufin O-deethylase assay (EROD), the Salmonella/microsome assay, and a gap junction intercellular communication (GJIC) assay were chosen to evaluate the toxic endpoints pertaining to three different stages of carcinogenesis induced by PAHs. Shape-electronic, spatial, information content and topological descriptors were important in the prediction of these endpoints. The study also predicted toxic equivalency factors (TEFs) for the chemicals. These toxicity estimates could be

incorporated in a toxicity assessment to complete a human health risk assessment for compounds where data are incomplete (Bruce et al., 2008).

Ying et al., (2006), used electrostatic potential calculations and geometric optimization at the HF/6-31 G level of theory (Zou) for the 209 PBDE congeners. Multiple linear regression method was used to model Henry's law constant (lg *H*), Ah receptor binding affinity (-lg RBA), 298 K supercooled liquid vapour pressures (lg p_L), n-octanol/air partition coefficient (lg K_{OA}) and gas-chromatographic relative retention time (RRT) against structural descriptors. The descriptors were derived from electrostatic potential and molecular volume. The equations have good predictive capabilities. Similarly, Harju et al., (2002), conducted a multivariate physicochemical characterization and QSPR designing for PBDEs to assess the risk they pose to human health and their fate. Molecular mechanics, semi-empirical method (AM1) and empirically estimated parameters were used to derive 40 descriptors that were further analyzed by principal component analysis. The descriptors included log *P* values, dipole moments, atomic charges, heats of formation, frontier molecular orbital energies and molecular surface areas. Partial least squares method was used with a set of 17 chemicals used for constructing the models.

Significance

QSAR modeling gives us statistically robust models that reduce time and cost of experimentation along with cutting down on hazardous waste produced. Thousands of descriptors are used to characterize the link between the structure of a compound and its biological activity. This research is aimed at designing QSAR

models for predicting toxic endpoints for a class of persistent organic pollutants in mammalian cells. These concepts and methods can be extended to other classes of compounds, or can be designed for a number of different endpoints working with different assays. These endpoints can be specific to a disease, a toxic endpoint, or a certain mechanism of action. This concept has a major application in the pharmaceutical industry, especially in drug discovery and design. The fundamental theory of QSAR modeling is based on the assumption that there is a relationship between the molecular and structural features of a compound and its biological activity. The aim of QSAR modeling is to characterize these relationships and extend the predictive model to the activity of new chemicals within the same family (Liu, 2005; Frimurer et al., 2000; Wagener et al., 2000; Liu, 2004). This, in effect, reduces the search for new drugs or shortens the process, making it more economical.

QSAR modeling is consistent with the three R's of sustainability: reduce, reuse, and recycle. QSARs reduce the amount of hazardous waste produced in experimentation. They can be reused to predict activity of compounds in the same family, and they can be recycled using additional toxicity information and descriptors to give another QSAR model to predict a different endpoint of interest.

There are, however, limitations to the feasibility, use, and application of QSAR methodology in modeling and predicting toxicity. Limitation of the availability and quality of the biological data is a primary constraint to the feasibility of this *in silico* tool. Compounds for which the activity is being

modeled need to have similar mechanism of action. The prediction is not very dependable for the chemicals that are beyond the chemical and mechanistic domain of the QSAR equation. For example, in the current study, QSAR designed for a training set with different kinds of flame retardants (and not just PBDEs) would not be very dependable because we are not sure whether each of them have the same mechanism of action. An attempt to model more complex endpoints is likely to have more restrictions and lesser reliability. The methods for determining the applicability domain for QSARs need development and refinement. More so, they are able to predict through interpolation only and not through extrapolation. This implies that a QSAR is able to predict for the structurally related chemicals within the domain of the training set only and not beyond it (Cronin, 2002).

QSARs are one of the several *in silico* tools that aid risk assessment and other researches that need toxicity data not available in the existing data bases or libraries. Testing for such data would need investment of enormous amount of time, manpower, skills, and resources. All of that can be saved if reliable models can be established for the more researched toxicological chemicals to fill up the information gaps. The basic utility of QSAR from an industrial perspective is that the toxicity predictions may be used to quantitatively determine risks from untested or unreliably tested chemicals. Hence, the manufacturers get information about the toxicity of a certain chemical in its developmental stage and its long term effects. Internationally, QSARs are used in regulatory contexts for screening applications. For example, the USEPA uses QSARs to screen industrial chemicals

to determine if they need to be tested. USEPA is interested in the possibility of combining traditional PBPK modeling with QSAR analysis to produce a protocol for high through-put screening processes for chemicals of concern. The QSAR paradigm found its earliest utility in the fields of agro chemistry then grew into pharmaceutical chemistry applications and today is used by almost every branch of chemistry (Suter et al., 2007).

Specific Objectives and Hypothesis

The specific aim of this research is to build QSAR models to predict specific toxic endpoints in mammalian cells due to exposure to PBDEs. The study is based on the hypothesis that QSARs are able to predict specific toxic endpoints, cell viability, oxidative stress, and apoptosis for PBDEs. The Janus Green assay was run to evaluate cell viability with Hep G2 cells. This assay provided the dose-response data for the PBDEs training set. The study used the Enzcheck Caspse assay to gather apoptosis data and the DCFH-DA assay to gather information regarding oxidative stress caused by PBDEs. Each of these sets of data were used to design three different QSAR models, one for each endpoint. In the final step the models were validated externally using compounds of interest from the same family (PBDEs) but not used for creating the models. These compounds used to validate the models are called the "test chemicals" and the ones used to create the models are referred to as the "training set chemicals".

To accomplish the QSAR modeling this study utilizes Discovery Studio® (DS; Accelyrs Inc, San Diego, CA, USA), a program that specializes in life

sciences research applications. With appropriate molecular descriptors, data found by experimentation were used to develop models to predict each of the endpoints of interest. Genetic function approximation algorithm, an analogy of DNA evolution was used for generating QSAR models. This protocol worked towards generating the best possible equations over thousands of generations of ranking bits of strings, pairing them and cross over operation to exchange descriptors between them. Molecular properties calculations was used for narrowing down the choice of descriptors at the preliminary stage. It generated statistics of numerical properties along with a correlation matrix of the available properties. It is one of the different general purpose protocols that enables finding out the appropriate descriptors and properties that can be derived from user-built QSAR models. It is also possible to generate new properties from already existing ones. If needed, the protocol can perform binning and fundamental correlation and statistical analysis on the various quantitative descriptors.

CHAPTER TWO

Methods

Cell Culture and Bioassays for Specific Endpoints

The human hepatocarcinoma cells (Hep G2) cells were purchased from American Type Culture Collection (ATCC, Manassas, VA). They were cultured in a simulated environment in an incubator at 37 ˚C and 5% CO_2. Eagle's minimum essential medium (from ATCC Manassas, VA or Sigma Aldrich, St. Louis, MO), was made into a complete growth medium by adding fetal bovine serum (from Atlanta Biologicals, Lawrenceville, GA) to a final concentration of 10% and was used for culturing the cells. The cells were seated in a 96 well plate at varying cell densities (3,000 to 11,000 per well) to check for the right density in a 72 hour study. The obtained optimum density was used to seat 96 well plates for cell viability studies. Cells were exposed to chemicals dissolved in 0.5% dimethyl sulfoxide (DMSO) (final concentration) for different incubation periods. Control cells were incubated with the vehicle (DMSO) only. The experimental plates had 16 replicates for each concentration of the dosed chemical. The treatments were experimented with PBDEs -19, -28, -47, -49, -99, -100, -153, -183, -190, -209, 3-OH-BDE-47, 5-OH-BDE-47, and 6-OH-BDE-47. The above chemical library was adopted from the flame retardant QSAR work by Harju et al., (2006). PBDEs -28, -47, -99, -100, -153, -183, -209, and the three hydroxy derivatives of PBDE-47 were used as the training set chemicals. Their selection was based on their occurrence in industrial products (Harju et al., 2006) and hence, their

environmental relevance. The chemicals were procured from AccuStandard (New Haven, CT, USA). Volumetric method was used to make up the stock solutions of the chemicals and their concentrations were analytically verified by gas chromatography mass spectrometry method. Hep G2 cells were stored in a -80˚C freezer for a short term and in liquid nitrogen for longer term storage when they were not being experimented with. Caspase-3 activity kits used for apoptosis rates study were purchased from Molecular Probes (Carlsbad, CA, USA).

Analytical Verification of Chemical Stock Solutions

The verification of PBDE standards' composition, purity, and their concentrations were determined using gas chromatography–mass spectrometry (GC/MS) on an Agilent 7890 GC coupled to an Agilent 5975 MS in electron capture negative ionization mode with selective ion monitoring. One microliter of a ~300 µL extract was injected on the column with an Agilent 7683 Injector in a pulsed splitless mode. The injection port temperature was 300 °C. Chromatographic separation was achieved using a DB-5ms capillary column (Agilent, 30m x 0.25 mm i.e.; 0.25µm film thickness). Helium (99.999%) was used as the carrier gas, and methane (99.999%) was the buffer gas. The oven temperature program started at 120° C, held for 1 min, ramped to 275° C at 4° C/min, then ramped to 320° C at 6°C/min, and held for the final 5 minutes. The total run time was 52.25 minutes. The ECNI's ion source and quadrupole mass analyzer temperatures were both set to 150°C. Target analytes were identified using retention times (±0.05 min) as well as quantitation and qualification ion ratios (±20%). Ion 79 m/z was used as the quantification ion for PBDEs (Usenko et al., 2011).

Determination of Cell Viability by Janus Green B

Janus Green is a basic dye used in histology and to stain mitochondria supravitally (Figure 2). The Janus Green B staining reaction depends on the oxygen content (Bensley, 1911, Bensley, 1938), for although selective staining of mitochondria appears under partial anaerobic conditions, these structures become decolorized when all of the oxygen is removed. The Janus Green B dyeing reaction on the cells is reversibly inhibited by cyanide (Lewis, 1923, Lewis and Lewis 1924); when cyanide is added to supravitally stained mitochondria they become colorless whereas when the cyanide is subsequently removed by washing, the mitochondria regain their blue color. Studies have shown that the dye is responsive to the lactic dehydrogenase enzyme system (Banga et al., 1933). From all of these studies, it can be concluded that Janus Green B staining is dependent on the enzyme activities of the cell.

The Janus Green dye was used to measure the cell viability. The cells were cultured in 96 well plates and were exposed to varying concentrations of the toxic chemical with 16 replicates for each concentration and incubated for a 24 hour period. This was followed by two PBS rinses following which the dye was applied to them for 60 seconds. The lysed cells were able to take up the dye as against the live ones giving a measure of cell toxicity under the effect of chemical exposure. Excess dye was removed by two PBS rinses. Ethanol (100 %) was used to extract the dye ready to be read. A measured volume of nanopure water was added to each well of the culture plate before it is read on the spectrophotometer to measure absorbance at 654 nm. A ELx800 absorbance

microplate reader by BioTek® (Winooski, VT, USA) was used to measure the optical density from the experimented plates.

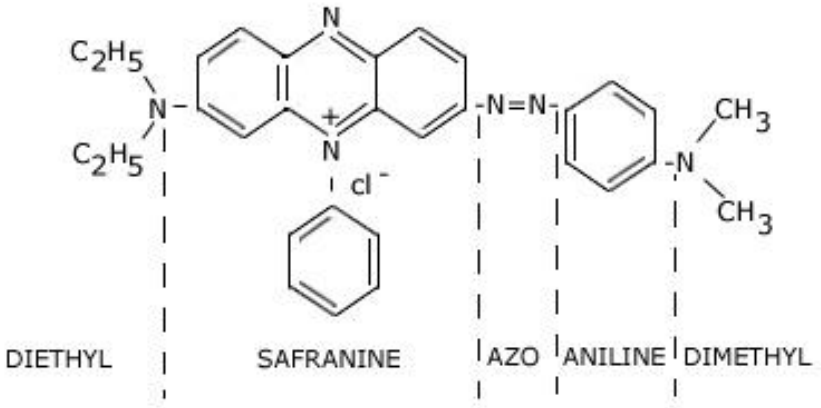

Figure 2. Structure of Janus Green. (Lazarow and Cooperstein, 2005)

Determination of Oxidative Stress by DCFH-DA

The theory behind using DCFH-DA is that hydrogen peroxide oxidizes nonfluorescent fluorescin derivatives and they emit fluorescence. This fluorescence emission is directly proportional to the concentration of hydrogen peroxide in the cell. The mechanism of action of DCFH-DA is illustrated in Figure 3. On applying to intact cells, the nonpolar, nonionic DCFH-DA crosses through the cell membranes and is hydrolyzed by intracellular esterases to nonfluorescent DCFH by enzyme action. In the presence of reactive oxygen species (ROS), mainly hydrogen peroxide, DCFH is oxidized to highly fluorescent dichlorofluorescein (DCF) (Wang et al., 1999). Therefore, the intracellular DCF fluorescence is a good determinant of the overall OS in cells.

Cells were split and counted and viable cells were seated in 96-well plates at a density of 100K cells per well two days prior to the experiment. They were

dosed with the chemicals, PBDEs and left for about 24 hours. Each experiment plate was dosed with five different concentrations of one PBDE congener, wherein, we had 16 replicates for each concentration. On the day of the experiment, after removing the medium, the cells in the plates were washed with PBS buffer and then incubated with 100 mM DCFH-DA in the loading medium (ACAS medium) in 5% CO_2/95% air at 37°C for 30 min. This step was carried out in dark. After removing the DCFH-DA, the cells were washed with PBS buffer and the fluorescence of the cells from each well was measured by the plate reader and recorded. A Fluoroscan Ascent FL® by Thermo Scientific (Watham, MA, USA) was used for recording the fluorescence signals at 485 ± 10 nm/ 530 ± 10 nm excitation vs. emission wavelengths.

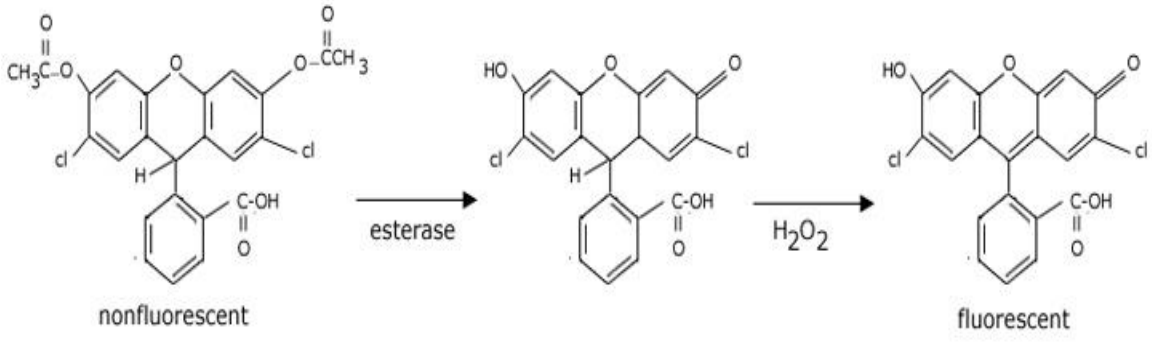

Figure 3. Mechanism of action of DCFH-DA. Adapted from Invitrogen® (Carlsbad, CA, USA) Molecular Probes handbook, product number D6883

Determination of Apoptosis by Caspase Assay

Apoptosis, or programmed cell death, is vital in development and in several states of a disease. It is both morphologically and biochemically different from the process of necrosis which is premature death of cells in the event of an

injury or accident. Unlike necrotic cells, apoptotic cells undergo shrinkage of the cytoplasm, compaction of nuclear chromatin and production of membrane-bound apoptotic bodies as their morphological characteristics. Biochemically, apoptosis, encompasses genome division and splitting or degradation of numerous cellular proteins as characteristics. In the recent past, members of the caspase (CED-3/ICE) family of proteases have been found to be important catalysts in the various complicated biochemical stages associated with apoptosis (Thornberry et al., 1998, Fisher et al., 1998). In particular, the activation of caspase-3 (CPP32/apopain), which has substrate specificity for the amino acid sequence Asp-Glu-Val-Asp (DEVD) and splits different proteins, including poly (ADP-ribose) polymerase (PARP), DNA-dependent protein kinase, protein kinase Cδ and actin is vital for the initiation of apoptosis (Fisher et al., 1998, Nicholson et al., 1995).

The EnzChek® Caspase-3 assay kit was used for the assessment of apoptosis by using an assay for increases in caspase-3 and other DEVD-specific protease activities (e.g., caspase-7). The fundamental for the assay is the 7-amino-4-methylcoumarin-derived substrate Z-DEVD–AMC (Figure 4) (where Z represents a benzyloxycarbonyl group), which is weakly fluorescent in the UV range (excitation/emission ~330/390 nm), but which yields a bright blue–fluorescent product (excitation/emission ~342/441 nm) upon proteolytic cleavage. The kit from Invitrogen® was used to monitor the activity of caspase-3 and closely related protease in cell extracts and purified enzyme preparations using a fluorescence microplate reader or fluorometer. Figure 5 illustrates the mechanism of action of capsase-3 in cleaving the two peptide links on the substrate Z-DEVD-R110.

Enzymes hydrolyze the first peptide link yielding fluorescent DCFH (monoamide R110) and highly fluorescent DCF (R110) on the next hydrolysis step. The fluorescence signal measured is assumed to be a direct measure of the extent of capsase-3 activity in the PBDE exposed cells. The fluorescence plate reader Fluoroscan Ascent FL® by Thermo Scientific (Watham, MA, USA) was used for recording the fluorescence signals at 485 ± 10 nm/ 530 ± 10 nm excitation vs. emission wavelengths.

Hepatocarcinoma (Hep G2) cells were cultured and seeded in 96 well plates @ 9K cells/well. They were dosed with varying concentrations of PBDEs 24 hours after seeding and incubated at 37 ˚C and 5% CO_2 for 72 hours. Each plate had 16 replicates for one concentration, one chemical per plate. 50 µl of cell lysis buffer was added in each well and the plates were incubated at -80˚C overnight. The lysate from individual wells was collected the following day and centrifuged. The supernatant was transferred to another micro plate. We added 50 µl of the substrate working solution (with Z-DEVD-R110) to each well and the plate was incubated at room temperature for 30 minutes. The fluorescence was then measured at 496nm/530nm excitation and emission.

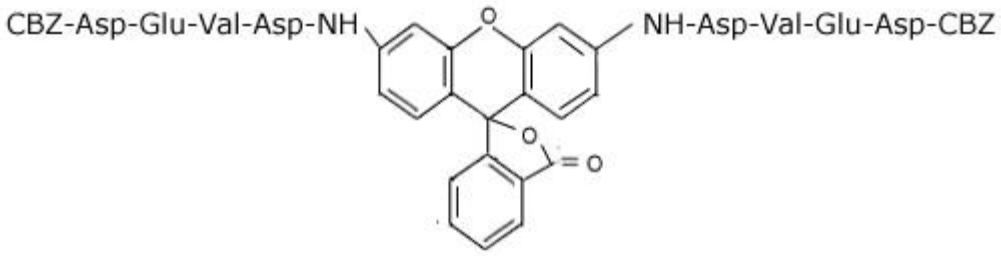

Figure 4. Bisamide derivative of Rhodamine 110 (Z-DEVD-R110, the substrate). Adapted from Invitrogen® (Carlsbad, CA, USA) Molecular Probes handbook, product number E13184

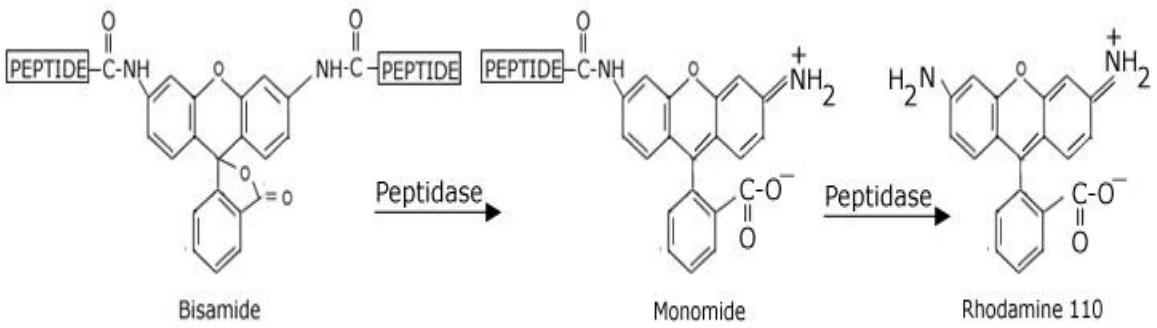

Figure 5. Mechanism of action of caspase-3 protease on Z-DEVD-R110 to highly fluorescent R110 in two steps. Adapted from Invitrogen® (Carlsbad, CA, USA) Molecular Probes handbook, product number E13184

Statistical Methods

Control and treatment levels were compared using one way analysis of variance with Tukey's test to determine significance ($p<0.05$) in JUMP (8.0 by SAS, Cary, NC, USA) and SigmaPlot 11.0 software (Systat Software, Inc., San Jose, CA). Dunnett's test was used to cross check the results from Tukey's test but has not been shown here. Assumptions for ANOVA; data sets from each experiment are normally distributed, groups in the set are independent and have homogeneous variances, were confirmed.

Building QSAR in Discovery Studio (Accelyrs Inc, San Diego, CA)

The experimentally determined endpoints for PBDEs from the above mentioned bioassays were used to construct QSAR models using genetic function approximation (GFA) method. For each congener tested for a set of experiment, the lowest observable adverse effect concentration (LOAEC) value was selected for modeling. This denotes the first indication of a significant toxic influence on

the cells. Responses at and above the modeled value can be considered to pose an unacceptable risk from a human health standpoint.

First, the chemical structures were entered into the program through SMILES (Simplified Molecular Input Line Entry Specification) codes generating a .sd file which is a chemical file format. The individual molecules were segregated into two groups, the training and the test sets. The structures could also be entered using building and sketching tools. The structures when entered in the program were in a crude form. They were refined by using prepare ligands protocol. This protocol was used to generate 3D structures and co-ordinates for the two files (groups), the training and test set chemicals. Prepare ligands protocol was used to generate tautomers and isomers, ionize functional groups, standardize charges for common groups, enumerate ionization states, add hydrogen atoms, remove duplicate structures, and retain only the largest fragments among other functions (Discovery Studio 2.5.5, 2010).

Molecular descriptors or the terms in which the QSAR equations were going to be defined were ascertained by calculate molecular properties protocol. The protocol helped find out the appropriate descriptors to characterize the dependent properties or activities, find their calculated values and develop a correlation matrix of all the descriptors. The least correlated descriptors were preferred over more correlated ones. Calculate molecular properties (CMP) has a library of different kinds of descriptors that are used to find the most appropriate ones relevant to the chemicals and the activity being modeled. The library consists of traditional molecular descriptors, semi-empirical QM descriptors, density

functional QM descriptors, topological descriptors, user defined descriptors, etc. The protocol is also able to derive new properties from two or more existing ones. It can perform binning operations to help reduce background noise and refine the descriptors. One important feature about CMP is that it generates statistics for all the numerical descriptors, which enables analysis and statistical comparison of all the descriptors.

The QSAR equations were generated by running the genetic function approximation protocol. Genetic function approximation (GFA) is, in effect, an analogy derived from the evolution of DNA. Individual biological entities were represented as strings of bits. The process of QSAR evolution started with a population of such random initial strings of bits. Ranking or scoring all the strings was done by a goodness of fit function called Friedman lack of fit (LOF) score. Friedman LOF tested the strings for their quality. The best fit combinations were paired together for developing a new generation by a crossover operation, so that only good genetic material from both parents was passed on to the offspring. This process of scoring, ranking, and mating of strings continued for several generations till the average fitness of the individuals in the population was raised. The final products had just good quality genetic material for further observation (Rogers and Hopfinger, 1993). GFA approach had several advantages over other methods. It generated a number of models together and not just one. It could build not just linear but higher order polynomials also. It did an automatic outlier removal by using splines. It was able to select the descriptors depending on the data set and the chemical structures, with conditions defined by the user. The user

however had discretion over a number of parameters in modeling. In the current study, GFA underwent 5000 generations to create 10 linear models. The initial and final equation lengths were selected to be 2 and 3 respectively, where initial equation length specified the minimum number of descriptors in the first generation and final equation length stood for the maximum number of descriptors. Linear splines were used to further refine the models. The user was able to specify the population size, i.e. the total number of models in the evolving population, 100 in this case. GFA used Friedman lack of fit score as a measure of goodness of fit which curtails over fitting (Rogers and Hopfinger, 1993) and gave a score to each model. Single score method was used to rank the models based on the outcome of the scoring done by Friedman's method.

The QSARs generated were validated for their predictive property through internal and external validation methods. Internal validation implies checking for good prediction among the training set chemicals themselves. Once the QSAR equations were calculated and verified by internal validation methods, they were used to predict the activity of compounds with unknown activity. This process is called "external validation" for which another set of PBDEs called the "test chemicals" was used. The entire chemical library of PBDEs was adopted from the QSAR work with brominated flame retardants by Harju el al., (2006). PBDEs -19, -49, and -190 were selected to be used as the test set. Their selection was based on the variation in their physicochemical properties (Harju et al., 2006) and their environmental relevance. The test chemicals' activity obtained through

experimentation was used to check how accurately the QSAR equations were able to predict.

CHAPTER THREE

Results

This section presents results from *in vitro* experiments for cell viability, oxidative stress, and apoptosis and the corresponding QSAR equations generated.It also tabulates the actual LOAEC values from the experimental results that were employed for generating the QSAR equations. The values predicted by the QSARs vs. those obtained from experiments have been graphically presented in this section. The statistical measures of the goodness of fit and goodness of prediction for the QSARs have also been presented.

Results from Analysis of Chemical Stock Solutions

The PBDE stock solutions were prepared by volumetric method and were analytically verified. All the concentrations obtained by the volumetric method were found to be within ±30% of calculated and prepared concentrations found by GC/MS analysis. This variability is considered acceptable for the GC/MS analysis that was conducted.

Toxicity Metric

Determination of LOAEC was one important step towards designing good QSAR models. Responses from bioassays were compared among each other for a significant difference ($p < 0.05$, Tukey's test). Control and solvent control (0.5% DMSO) were checked first for significant differences. No significant difference meant the solvent did not interfere with the responses elicited by the treatment

chemicals (Cell Viability ≥ 85%). Then the solvent control was statistically compared with each of the responses from treatments at increasing concentration. The lowest concentration that was significantly different from the solvent control was used as the experimental LOAEC value and was incorporated into the model. This value represents the lowest concentration of the chemical that elicits a significant toxic response among the concentrations tested. The LOAEC was used rather than a NOAEC because of the experimental design constraints of *in vitro* work. Time, cell growth, proliferation times, and cost limited the number of concentrations that could be run within the allotted time frame. This resulted in some cases where a NOAEC was not observed in the concentration ranges tested. In future, if these models were to be expanded to estimate a NOAEC, a larger concentration range would be examined including lower concentrations to determine a NOAEC.

All the experiments were conducted at 0.5% DMSO concentration. This percent solvent was determined from an experiment run using different concentrations of DMSO (0.1%, 0.3%, 0.5%, 0.7%, and 1.0%). Cells were dosed for 24 hours and checked for cell viability (85% minimum).. The percentage DMSO that did not cause a significant difference in cell viability was then used for comparision of treated cells and control by Tukey's test. This was done to ensure that the solvent does not interfere with the effect of the treatment chemical. If there was a statistically significant difference found between the two ($p < 0.05$, Tukey's test), the results were discarded and rerun. Hence, all of the

results presented come from experimental plates that had no significant difference between control and solvent control.

Figure 6 below shows the comparative responses of a cell viability assay to different parent PBDE congeners. The results represent the percentage of cells surviving the influence of the increasing nominal concentration of the toxic chemical. The error bars represent the standard error about the mean. There was no statistically significant difference found between controls and solvent controls for the experiments.

PBDE -28, -47, -99, and -183 showed statistically significant decreases in cell viability in a dose dependent manner. PBDE -209 showed significant reductions in percentage viability dose dependently up to 5mg/l. PBDE -153 did not show any significant decreases in percentage cell viability, whereas BDE -100 was significantly different from controls at only the 10mg/l treatment level.

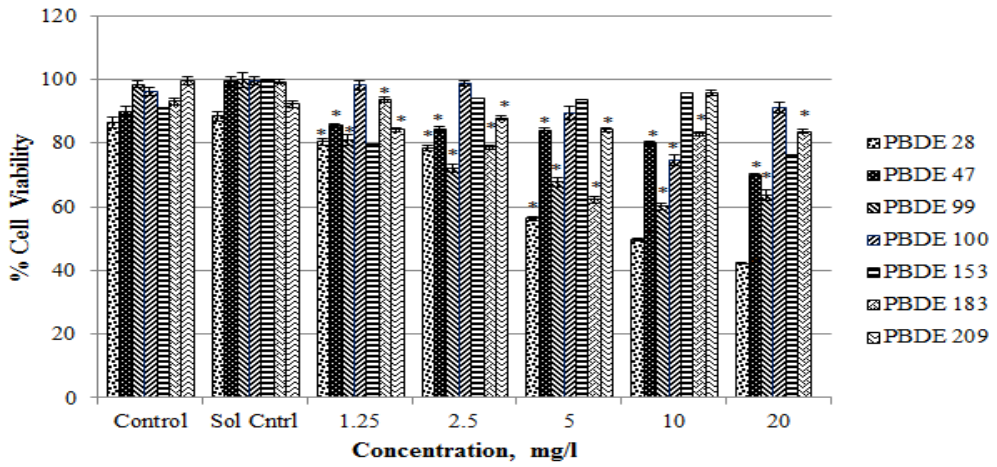

Figure 6. Percentage viability of Hep G2 cells exposed to different nominal concentrations (0, 1.25, 2.5, 5.0, 10.0, 20.0 mg/l) of PBDE parent congeners and a solvent control group (0.5% DMSO). Data are presented as percentage viability (n=16) ± SEM. Asterix indicates statistically significant difference from solvent control (*p< 0.05, Tukey's test). Control and solvent control were not significantly different (p< 0.05, Tukey's test).

Figure 7 below illustrates dose response relationships for hydroxylated PBDE congeners in a cell viability assay. The results in Figure 7 represent the percentage of cells continuing to proliferate upon being exposed to the increasing nominal concentration of the toxic chemical. The error bars represent the standard error about the mean.

PBDE -47 and 6-OH-PBDE-47 showed statistically significant decreases in cell viability in a dose dependent manner. 5-OH-PBDE-47 showed significant decreases only at high nominal concentrations (i.e.,10 mg/l, 20 mg/l), whereas 3-OH-PBDE-47 did not show significant decreases in percentage cell viability.

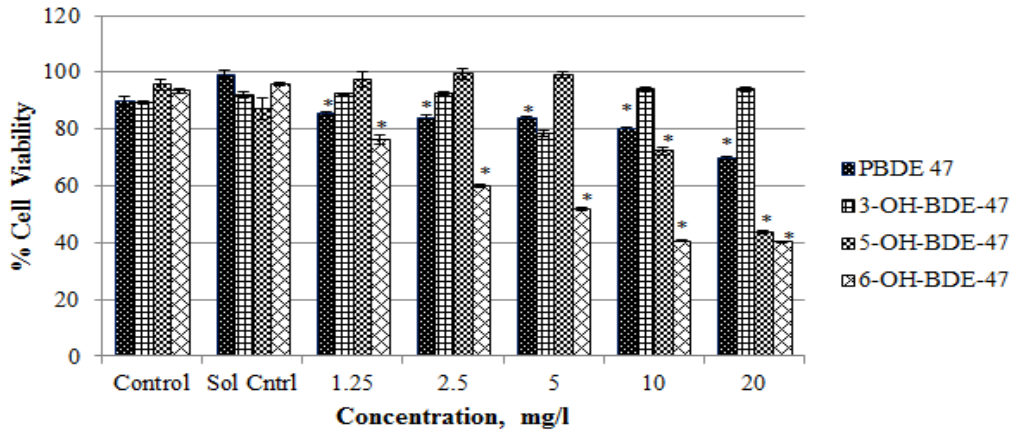

Figure 7. Percentage viability of Hep G2 cells exposed to different nominal concentrations (0, 1.25, 2.5, 5.0, 10.0, 20.0 mg/l) of PBDEs hydroxylated congeners and a solvent control (0.5% DMSO). Data are presented as percentage viability (n=16) ± SEM. Asterix indicates statistically significant difference from solvent control (*p< 0.05, Tukey's test). Control and solvent control were not statistically different (p< 0.05, Tukey's test).

The chart in Figure 8 below is an interpretation of the percentage of cells that were able to survive the fatal influence of the toxicants upon a 72 hour exposure. The error bars stand for the standard error about the mean. PBDE -19,

-49, and -190 did not show a statistically significant effect on Hep G2 cell viability at any of the doses at varying nominal concentrations. These chemicals were used as test chemicals to verify the model predictions.

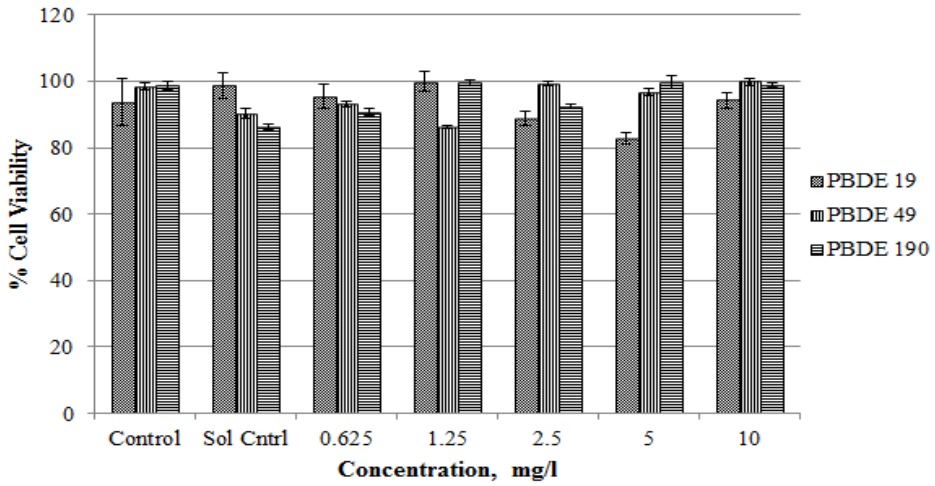

Figure 8. Percentage viability of Hep G2 cells exposed to varying nominal concentrations (0, 0.625, 1.25, 2.5, 5.0, 10.0 mg/l) of PBDE congeners to be used as test chemicals and solvent control (0.5% DMSO). Data are presented as percentage viability (n=16) ±SEM. Asterix indicates statistically significant differences compared with solvent control (*p< 0.05, Tukey's test). The difference of the response between control and solvent control are not statistically significant (p< 0.05, Tukey's test).

The following Figure 9 represents a regression of predicted log toxicity versus experimental log toxicity for the training set chemicals. The regression gives a coefficient of determination R^2 value of 0.973. Figure 10, similarly, represents the predicted values plotted against the observed values for the test set chemicals, the regression giving an R^2 0.827. The regression performed gave a p-value of 1.245e-006.

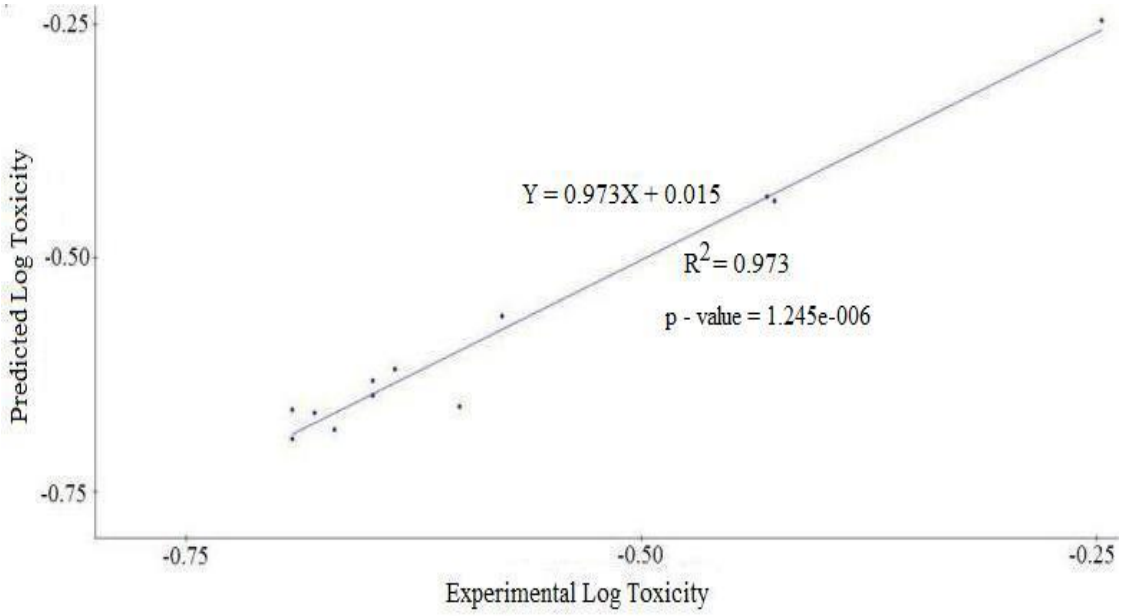

Figure 9. QSAR for cell viability responses elicited by the training set chemicals. Predicted log toxicity (absorbance intensity) versus experimental log toxicity (absorbance intensity).

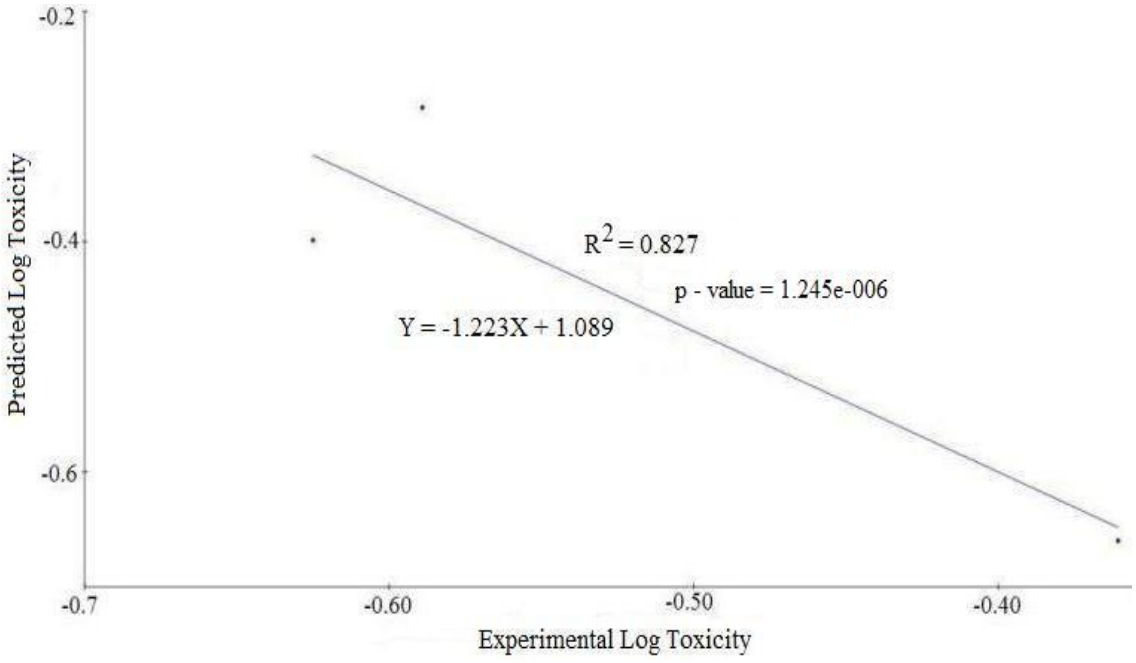

Figure 10. Validation run for cell viability QSAR. Plot of values predicted by Discovery Studio against cell viability responses elicited by the test set chemicals. Predicted log toxicity (absorbance intensity) versus experimental log toxicity (absorbance intensity).

For the oxidative stress experiments, cells were subjected to 100 µl/well of DCFH-DA in solution with media at 10.0 µM concentration. Each experiment was run in duplicate with n = 16 for every treatment. The results represent the percentage of oxidative stress caused in the cells due to ROS production upon exposure to each PBDE congener at different dose levels for a 24 hour interval. The error bars represent the standard error about the mean.

According to Figure 11, PBDE-47 induced maximum oxidative stress because it showed a significant 90% oxidative stress increase, highest among all the congeners tested at a low nominal concentration (2.5 mg/l). PBDE-47 caused a 70% increase in oxidative stress at 1.25 mg/l and a 50% increase when dosed at 5.0 mg/l. PBDE -183 also showed significant increase at lower nominal concentrations (i.e., 1.25 mg/l, 2.5 mg/l). PBDE -153 and -209 showed significant increases in ROS production at 5.0, 10.0, and 20.0 mg/l in a dose-dependent manner. PBDE -99, on the other hand, had significant effects only at the highest two doses tested (i.e., 10.0 and 20.0 mg/l). PBDE -28 and -100 showed significant effects on the percentage oxidative stress increase only at 20.0 mg/l dosage. Cells were treated with 100 µl/well of DCFH-DA in solution with media to get a 10.0 µM final concentration on the cells. The experiment was conducted twice for each chemical with 16 replicates. The results represent the percentage oxidative stress increase in cells upon exposure to each PBDE congener at varying nominal concentrations for a 24-hour span. The error bars stand for the standard error about the mean.

6-OH-PBDE-47 induced significant oxidative stress in the cells dose dependently with a high 50% oxidative stress increase when dosed at 5.0 mg/l (Figure 12). PBDE-47 showed a 90% increase in the observed oxidative stress but only at lower nominal concentrations (i.e., 1.25-5.0 mg/l). 5-OH-PBDE-47 had significant effects only at 20.0 mg/l, whereas 3-OH-PBDE-47 had no significant effects on the oxidative stress in Hep G2 cells. PBDE – 47 represented as underneath shows a significant difference between control and solvent control. The two means were checked through the ANOVA and were found to have no significant difference between them.

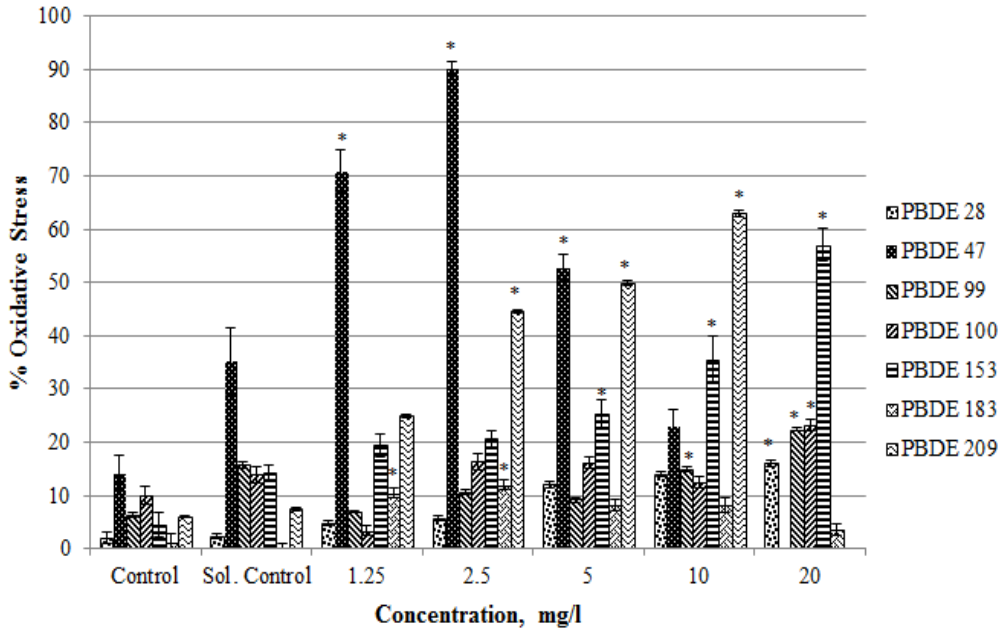

Figure 11. Percentage oxidative stress in Hep G2 cells exposed to different nominal concentrations (0, 1.25, 2.5, 5.0, 10.0, 20.0 mg/l) of parent PBDE congeners. The solvent control group was dosed with 0.5% DMSO. Data are presented as percentage oxidative stress (n=16) ± SEM. Asterix indicates statistically significant differences compared with solvent control (*p< 0.05, Tukey's test). The control and solvent control were not significantly different (p< 0.05, Tukey's test).

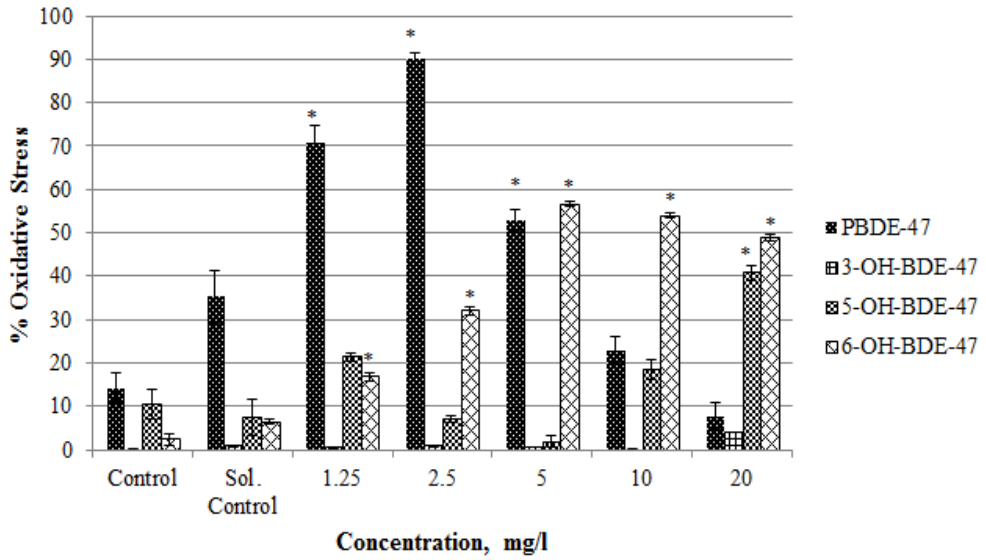

Figure 12. Percentage oxidative stress in Hep G2 cells exposed to different nominal concentrations (0, 1.25, 2.5, 5.0, 10.0, 20.0 mg/l) of hydroxylated PBDE congeners. The solvent control group was dosed with 0.5% DMSO. Data are presented as percentage oxidative stress (n = 16) ± SEM. Asterix indicates statistically significant differences compared with solvent control (*p< 0.05, Tukey's test). The control and solvent control were not significantly different (p< 0.05, Tukey's test).

Cells were treated with 10.0 µM of DCFH-DA in solution with DMSO at a volume of 100 µl/well. The experiment was run in duplicates with n = 16 for each treatment. The results represent the percent oxidative stress caused in the cells (with respect to the solvent control) due to ROS production upon exposure to each PBDE congener at different dose levels for 24 hours. The error bars signify the standard error about the mean.

Figure 13 shows that PBDE-190 had a significant effect on the percentage increase in oxidative stress in Hep G2 cells dose dependently up to 5.0 mg/l. PBDE-49 had significant effects on the cells only at 10.0 mg/l, whereas PBDE-19 significantly increased the oxidative stress when dosed at 1.25 and 2.5 mg/l.

These chemicals and the observations below served as a tool to externally validate the generated QSAR models.

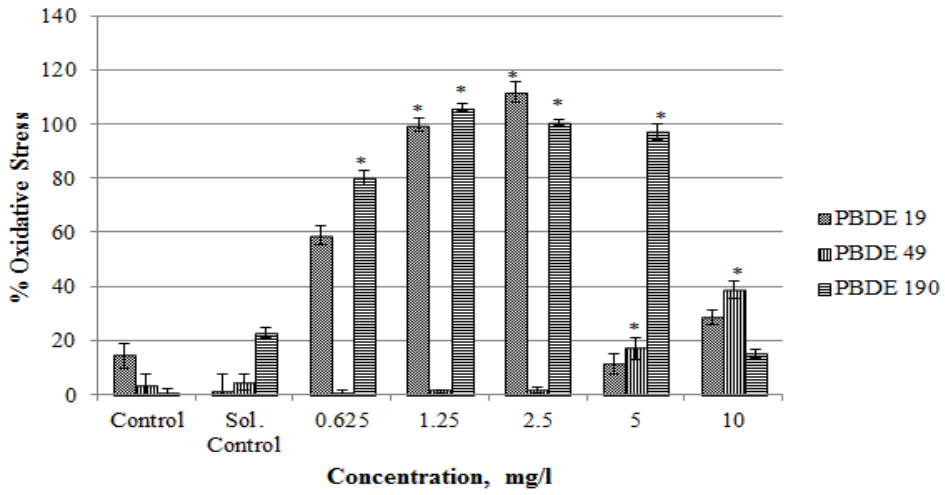

Figure 13. Percentage oxidative stress in Hep G2 cells exposed to different nominal concentrations (0, 1.25, 2.5, 5.0, 10.0, 20.0 mg/l) of PBDE congeners (test chemicals). The solvent control group was dosed with 0.5% DMSO. Data are presented as percentage oxidative stress (n=16) ± SEM. Asterix indicates statistically significant differences compared with solvent control (*p< 0.05, Tukey's test). The control and solvent control were not significantly different (p< 0.05, Tukey's test).

Figure 14 represents a plot of the predicted log oxidative stress values versus the observed ones for the training set chemicals. The regression gives a coefficient of determination, R^2 of 0.922. Figure 15 similarly gives a representation of the predicted log oxidative stress versus the observed value for the test set chemicals, with an R^2 of 0.905. The p-value for the performed regression is 1.033e-005.

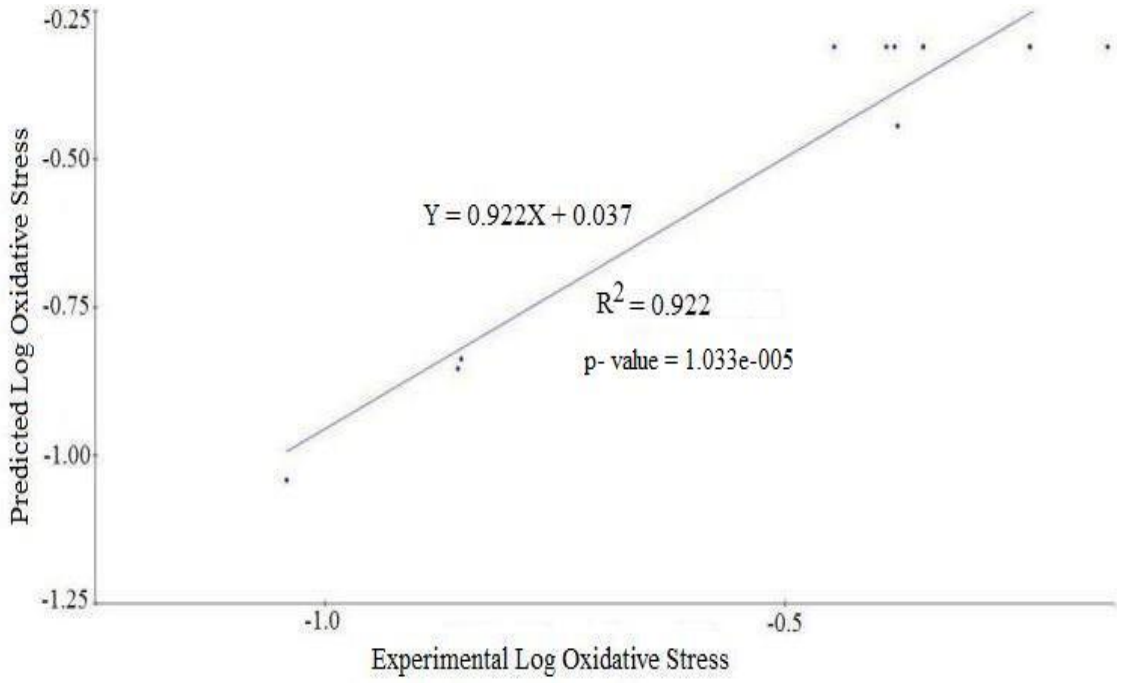

Figure 14. QSAR for oxidative stress responses elicited by the training set chemicals. Predicted log oxidative stress (fluorescence intensity) versus experimental log oxidative stress (fluorescnce intensity).

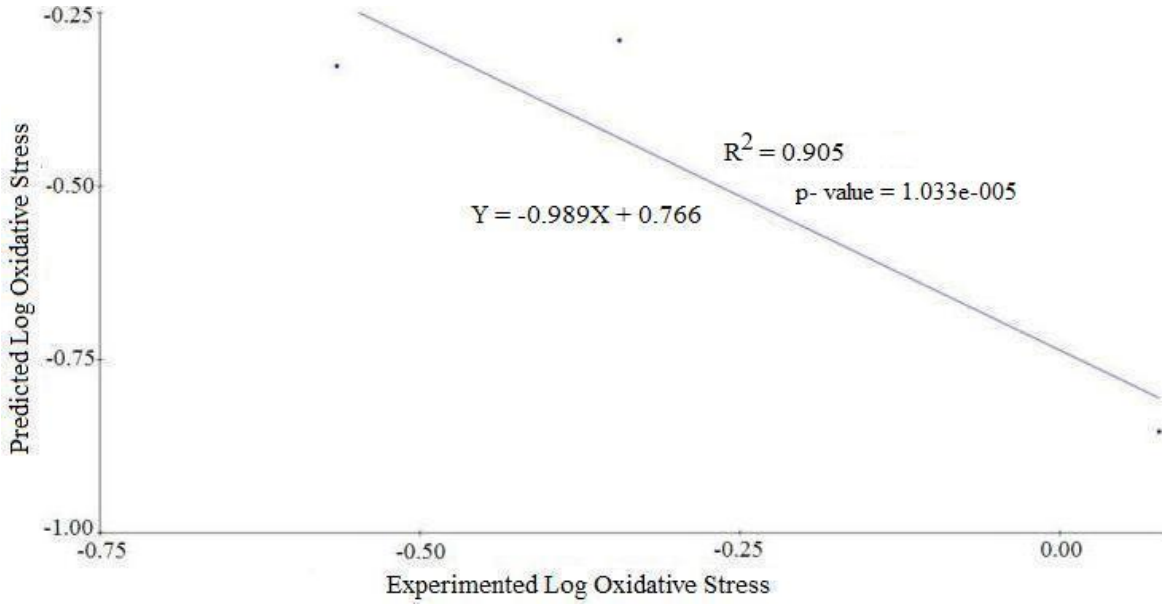

Figure 15**.** Validation run for oxidative stress QSAR. Plot of the values predicted by Discovery Studio against responses elicited by the test set chemicals. Predicted log oxidative stress (fluoroscence intensity) versus experimental log oxidative stress (fluoroscence intensity).

The rates of apoptosis that Hep G2 cells underwent upon being exposed to PBDEs for 72 hours were estimated by measuring caspase-3 protease activity. Experiments were carried out two times with n=16 for each nominal concentration of individual congeners. The results represent the percentage of cells that showed signs of cellular injury in the form of caspase-3 activity upon being exposed to varying nominal concentrations of the toxic chemicals. The error bars signify standard error about the mean for each treatment.

It was observed (Figure 16) that PBDE -100 induced significant caspase-3 activity in the cells in a dose dependent manner, effective at 2.5, 5.0, 10.0, and 20.0 mg/l nominal concentrations. PBDE -47 and -183 had significant effects only when dosed at 10.0 mg/l. PBDEs -47, -100, and -209 gave a normal response (bell shaped curve) to increasing amounts of dosage, the experiment being performed under identical conditions.

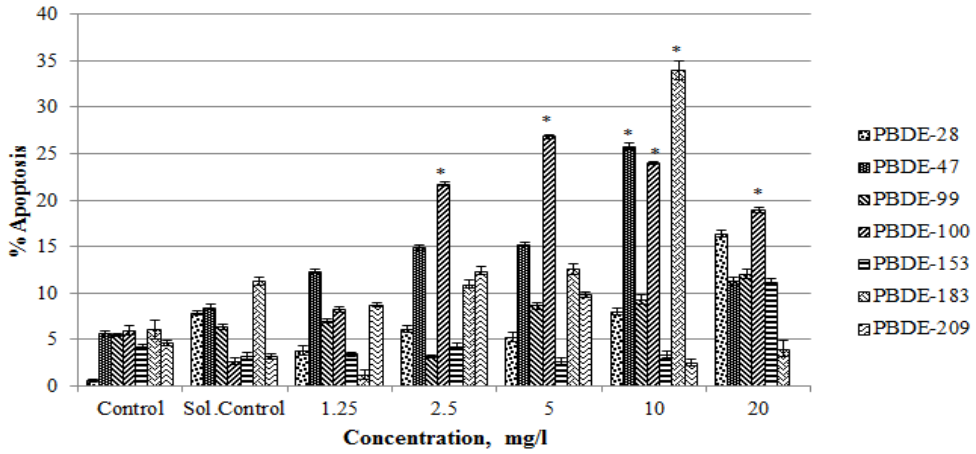

Figure 16. Percentage caspase-3 activity responses in Hep G2 cells exposed to different nominal concentrations (0, 1.25, 2.5, 5.0, 10.0, 20.0 mg/l) of parent PBDE congeners. The solvent control group was dosed with 0.5% DMSO. Results are presented as percentage apoptosis (n=16) ± SEM. Asterix indicates statistically significant differences compared with solvent control (*p< 0.05, Tukey's test). The control and solvent control were not significantly different (p< 0.05, Tukey's test).

The rates of apoptosis that Hep G2 cells underwent upon being exposed to varying nominal concentrations of PBDEs were estimated by measuring the caspase-3 protease activity. The experiment was run two times for each congener with 16 replicates for each treatment. The results represent the percentage of cells that experienced an injury read as the caspae-3 activty upon being exposed to increasing nominal concentrations of the toxic chemical for a 72 hour interval. The error bars are a representation of the standard error about the average for each nominal concentration.

A dose-dependent response was observed with 6-OH-PBDE-47 starting at 2.5, up to 20.0 mg/l nominal concentration, with the caspse-3 activity showing a 100% apoptosis increase with respect to the solvent control at higher nominal concentrations. 5-OH-PBDE-47 had significant effects only at high nominal concentrations, 10.0 and 20.0 mg/l. The hydroxylated PBDE congeners displayed up to four times greater response as compared to the parent congener as can be seen in Figure 17.

There was a separate comparison done for the hydroxylated congeners than the different parent congeners. This was done to assess the effect of hydroxylation on the parent PBDE congener (PBDE-47 for the current study). In most studies, 6-hydroxylated-PBDE- 47 was found to induce most toxicity followed by 5-hydroxylated-PBDE-47 than the parent PBDE-47 congener. 3-hydroxylated-PBDE-47 congener was not found to induce significant toxicity. 6-OH-BDE-47 has the hydroxy group in the ortho position with relation to the ether linkage. This is responsible for the high toxicity induced according to our hypothesis.

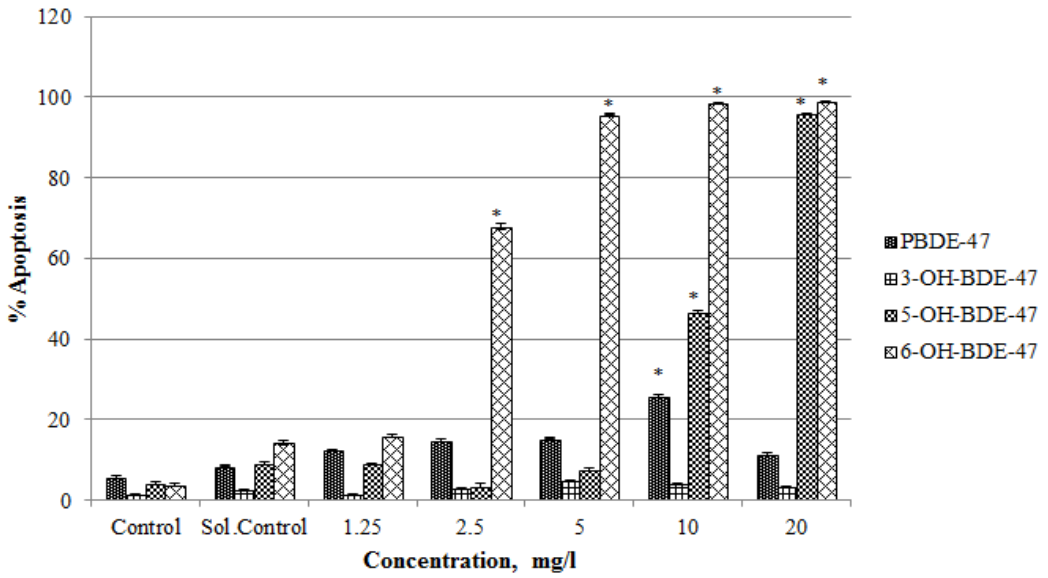

Figure 17. Percentage caspase-3 activity responses in Hep G2 cells exposed to different nominal concentrations (0, 1.25, 2.5, 5.0, 10.0, 20.0 mg/l) of hydroxylated PBDE congeners. The solvent control group was dosed with 0.5% DMSO. Results are presented as percentage apoptosis (n=16) ± SEM. Asterix indicates statistically significant differences compared with solvent control (*p< 0.05, Tukey's test). The difference between control and solvent control responses were not significantly different (p< 0.05, Tukey's test).

The rates of apoptosis that Hep G2 cells undergo upon being exposed to varying nominal concentrations of PBDEs for 72 hours were estimated by measuring the caspase-3 protease activity. The experiments were run in duplicates with n=16 for each nominal concentration. The results represent the percentage of cells that underwent caspase-3 activity upon being exposed to increasing nominal concentrations of the toxic chemical for a 72-hour period. The error bars represent standard error about the mean. These chemicals were used as test chemicals to externally validate the QSAR model created. PBDE-19 elicited a significant 23% caspase-3 activity upon being dosed at 5 mg/l nominal concentration. A significant

37% caspase-3 activity was observed with PBDE-190 at 10 mg/l dosage (Figure 18).

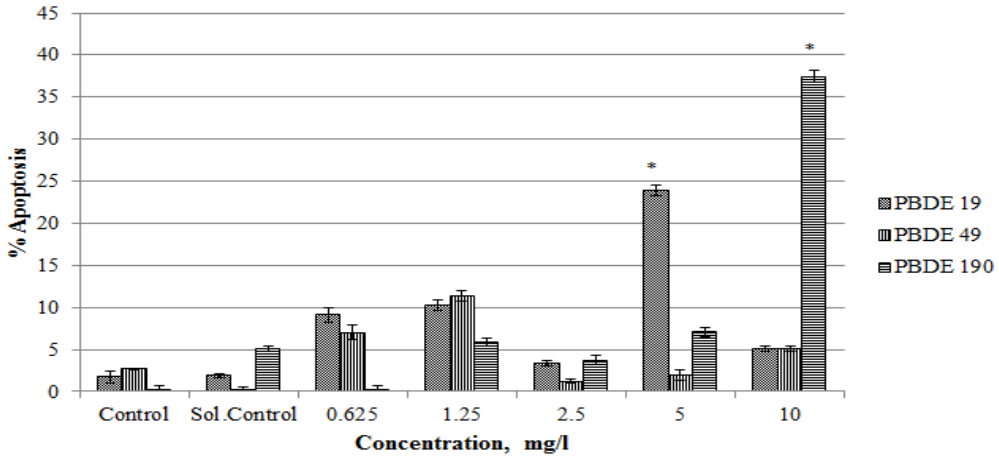

Figure 18. Percentage caspase-3 activity responses in Hep G2 cells exposed to different nominal concentrations (0, 1.25, 2.5, 5.0, 10.0, 20.0 mg/l) of PBDE congeners (test chemicals). The solvent control group was dosed with 0.5% DMSO. Results are presented as percentage apoptosis (n=16) ± SEM. Asterix indicates statistically significant differences compared with solvent control (*p< 0.05, Tukey's test). The control and solvent control responses were not significantly different (p< 0.05, Tukey's test).

The following Figure 19 represents predicted log apoptosis values plotted against the observed ones for the training set chemicals. The regression gives a coefficient of determination, R^2 of 0.939. Figure 20 similarly gives a representation of the predicted log apoptosis versus the observed value for the three test set chemicals, with an R^2 of 0.812. The p-value for the performed regression is 3.258e-005.

Table 1 details the responses from in vitro experiments that were modeled to generate QSAR equations. These responses correspond to the LOAEC doses in the dose response curves for each of the bioassay experiments (Toxicity Metric section).

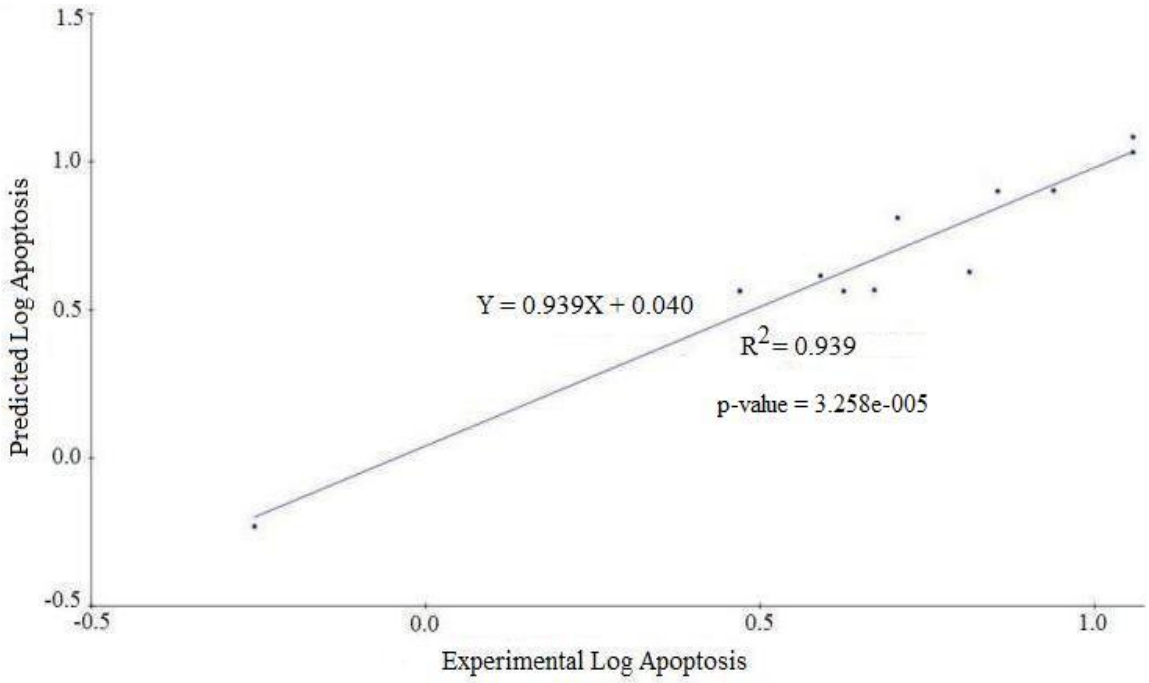

Figure 19**.** QSAR for the caspase-3 activity responses elicited the training set chemicals. Predicted log apoptosis (fluoroscence intensity) versus experimental log apoptosis (fluoroscence intensity).

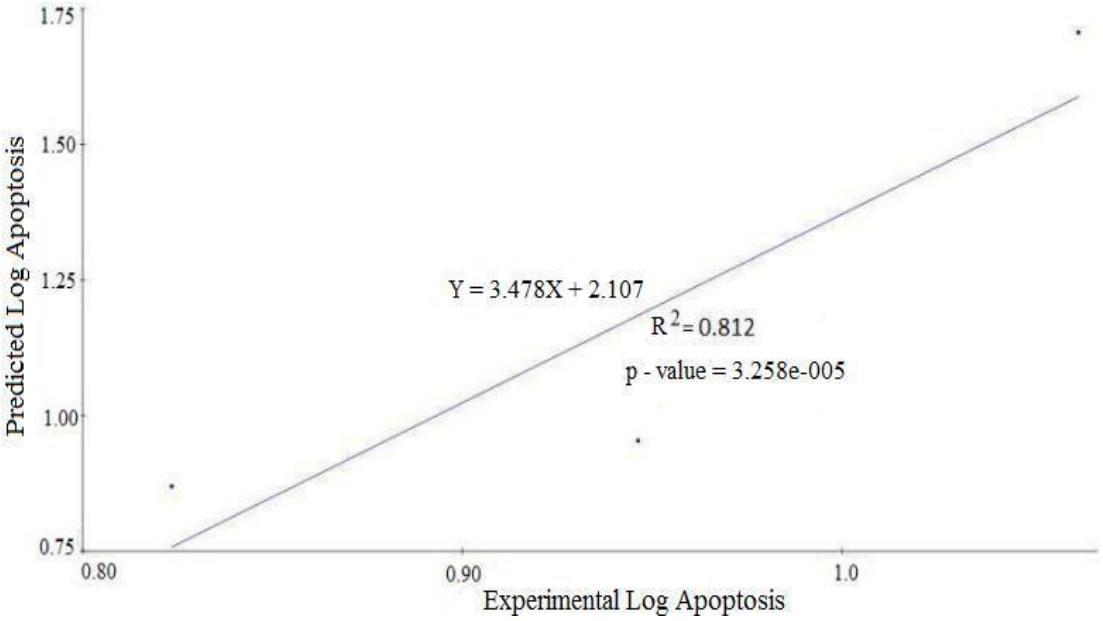

Figure 20. Validation run for caspase-3 activity QSAR. Plot of the values predicted by Discovery Studio against responses elicited by the test set chemicals. Predicted log apoptosis (fluoroscence intensity) versus experimental log apoptosis (fluoroscence intensity).

The equations following Table 1 represent the QSARs designed for the three sets of data, cell toxicity, oxidative stress, and apoptosis described in the figures above. For each data set, there were a total 10 QSAR equations generated. One was selected from the best three on the basis on Friedman LOF score and the r^2. The highest r^2 and the lowest LOF score represent a well-trained model that has not been overfitted and predicts reliably. Table 2 enumerates the related statistical data for the three equations. The final three QSAR equations designed for the three endpoints are represented graphically in Figures 9, 14, and 19 respectively. External validation for the three equations was conducted with three test chemicals. Equations 2, 3, and 4 were able to predict the activity for the test chemicals with an r^2 of 0.827, 0.905, and 0.812, respectively. The regression performed for external validation of the models is shown in Figures 10, 15, and 20, respectively. ALogP_AtomScore and ALogP_AtomMRScore belong to the ALogP family of molecular descriptors and are mentioned in the QSAR equations developed (equations 3 and 4). AlogP is the hydrophobicity of a molecule calculated by an atom based method postulated by Crippen and Ghose(1986). It is an important descriptor in QSAR equations since it indicates the extent of bioavailability of a chemical and the uptake of a xenobiotic by tissues. Hence it is an important biomarker that leads to prediction of cytotoxicity endpoints. ALogP_AtomScore is each individual atom's contribution towards the molecular ALogP. ALogP_AtomMRScore is similarly each atom's contribution towards the molar refractivity or polarizability of the molecule. Polarizability is a measure of the change in a molecule's electron distribution when it interacts with another

molecule of a reagent or solvent. It is a property of matter and deals with the internal structure of the molecule.

Table 1. Lowest observable adverse effect concentration (LOAEC) values from invitro experiments used for generating QSAR equations

Chemical↓ Experiment→	Cell Viability (Absorbance Intensity)	Oxidative Stress (Fluorescence Intensity)	Apoptosis (Fluorescence Intensity)
PBDE - 28	0.231563	0.139419	8.687625
PBDE - 47	0.25125	0.416013	5.076438
PBDE - 99	0.374188	0.140581	3.894313
PBDE - 100	0.370688	0.357669	6.502875
PBDE - 153	0.565938	0.407706	7.166438
PBDE - 183	0.265125	0.419238	4.68775
PBDE - 209	0.2145	0.090813	0.555025
3-OH-PBDE - 47	0.22515	0.447075	11.41813
5-OH-PBDE - 47	0.209188	0.709525	4.216813
6-OH-PBDE - 47	0.203375	0.583969	2.95
PBDE - 19	0.435813	0.367313	11.54056
PBDE - 49	0.237125	0.33526	6.659688
PBDE - 190	0.257563	0.272319	8.836688

QSAR Equations

$$\text{Log\_Toxicity} = -0.90321 - 2.0635 * \text{Gasteiger\_Charges} + 0.0073731 * \text{VSA\_AtomicAreas} + 0.0052213 * \text{VSA\_PartialCharge} \quad (2)$$

Log_OS = -1.368 + 1.0999 * ALogP_AtomScore

+ 13.731 * Gasteiger_Charges (3)

Log_Apoptosis = 7.5019 – 0.18962 * ALogP_AtomMRScore

– 1.9773 * Kappa_3+ 0.014776 * VSA_PartialCharge (4)

Table 2**.** Relevant statistics for the developed QSARs

	r^2	r^2 (adj)	r^2 (pred)	Friedman LOF	RMS residual error	SOR p-value
Log_Toxicity	0.9733	0.9632	0.9400	0.003245	0.0266	1.245e-006
Statistic→ Endpoint↓	0.9220	0.9047	0.7384	0.01674	0.08777	1.033e-005
Log_Apoptosis	0.9393	0.9165	0.8536	0.1021	0.04782	3.258e-005

Log_OS

Gastieger charges (equations 2 and 3) is another atom-based property where each atom of the molecule gets designated with a calculated partial charge on Pauling's scale. Van der Waal's surface area (VSA) variants figure as important descriptors in the generated QSARs (equations 2 and 4). VSA_AtomClass is a measure of each individual atom's contribution towards the total surface area of the molecule. VSA_PartialCharge which, on the other hand, calculates the surface area of the molecule based on the atomic partial charges. Kappa 3 is another descriptor that is important for modeling caspase-3 activity responses (equation 4). It is a two-dimensional shape descriptor used to quantify the topology of a

molecule. Kappa indices describe size, cylicity, and branching of the molecular structure (Hu. et al., 2004).

The following tables (3, 4, and 5) present the statistics for the Analysis of Variance (ANOVA) run as a measure to check any significant difference between the control and the solvent control for the experiments. Table 3 shows the results for cell viability experiments, Table 4 for oxidative stress, and Table 5 are the results for the apoptosis experiments. An alpha $\alpha = 0.05$ was assumed. Each of the following tables contain two ANOVA runs, the first one for control and solvent control and the second one for solvent control and the treatments. A p-value< 0.05 signified a significant difference between the means that were compared and a p-value> 0.05 signified no significant difference between them. Looking at the statistics on Tables 3, 4, and 5, we can tell that the control and the solvent control were not significantly different with respect to each other. On the contrary, there was significant difference observed when the solvent control was compared to the different treatments. ANOVA would not be able to tell us exactly where the siginificant difference lies between the means. That is the reason why Tukey's test was used to compare all the means to find out the response from which of the treatments was significantly different with respect to the solvent control. A significant difference between the control and the solvent control indicated an interference in the observations because of the solvent or carrier. Data from plates with a significant difference between control and solvent control were not considered for analysis and then modeling.

Table 3. Relevant ANOVA statistics for cell viability studies

Endpoint	Cell Viability					
Comparison	Control and Sol. Control			Sol. Control and treatments		
Chem ↓ Stats →	N	F - stat	p-value	N	F - stat	p-value
PBDE - 28	8	2.878773	0.111865	16	56.81516	3.27E-25
PBDE - 47	8	0.008018	0.92992	16	11.04162	3.79E-08
PBDE - 99	8	0.935019	0.349971	16	5.657927	0.000157
BDE - 100	8	0.007815	0.930809	16	4.045398	0.002483
PBDE - 153	8	0.436464	0.519558	16	1.330426	0.001859
PBDE - 183	8	0.022222	0.883624	16	15.41681	1.15E-10
PBDE - 209	8	1.382558	0.259275	16	6.517038	3.77E-05
3-OH-BDE-47	8	1.684044	0.215363	16	8.710034	1.17E-06
5-OH-BDE-47	8	0.649907	0.433627	16	14.44014	3.92E-10
6-OH-BDE-47	8	2.091512	0.170135	16	50.71747	1.11E-23
PBDE - 19	8	0.004841	0.945512	16	1.647602	0.156708
PBDE - 49	8	1.718773	0.210949	16	4.493592	0.001141
PBDE - 190	8	6.68522	0.061574	16	1.610796	0.166378

Table 4. Relevant ANOVA statistics for oxidative stress studies

Endpoint	Oxidative Stress					
Comparison	Control and Sol. Control			Sol. Control and treatments		
Chem ↓ Stats →	N	F - stat	p-value	N	F - stat	p-value
PBDE - 28	8	0.122732	0.731305	16	2.535629	0.034785
PBDE - 47	8	0.791047	0.388811	16	8.727957	1.14E-06
PBDE - 99	8	11.14515	0.064875	16	3.56837	0.005714
BDE - 100	8	2.514533	0.135123	16	5.662559	0.000156
PBDE - 153	8	6.036032	0.077677	16	6.451872	4.2E-05
PBDE - 183	8	4.940677	0.083214	16	14.8058	2.46E-10
PBDE - 209	8	2.932564	0.108859	16	9.952202	1.82E-07
3-OH-BDE-47	8	0.01876	0.893007	16	1.509777	0.195779
5-OH-BDE-47	8	0.20103	0.660751	16	15.99553	5.62E-11
6-OH-BDE-47	8	8.906885	0.059851	16	373.6832	7.23E-55
PBDE - 19	8	0.000621	0.980474	16	14.07063	6.3E-10
PBDE - 49	8	0.216058	0.649207	16	12.06736	9.06E-09
PBDE - 190	8	0.984252	0.337989	16	9.088874	6.59E-07

Table 5. Relevant ANOVA statistics for apoptosis studies

Endpoint	Apoptosis					
Comparison	Control and Sol. Control			Sol. Control and treatments		
Chem ↓ Stats →	N	F - stat	p-value	N	F - stat	p-value
PBDE - 28	8	5.542826	0.063685	16	5.156622	0.000366
PBDE - 47	8	0.754162	0.399804	16	1.208202	0.003126
PBDE - 99	8	0.938715	0.34905	16	2.90064	0.018408
BDE - 100	8	0.084722	0.775265	16	0.595527	0.007034
PBDE - 153	8	0.174383	0.682579	16	2.451075	0.040277
PBDE - 183	8	1.472954	0.244959	16	2.255287	0.056451
PBDE - 209	8	0.027075	0.871655	16	3.888296	0.003266
3-OH-BDE-47	8	0.286111	0.601116	16	0.805585	0.548946
5-OH-BDE-47	8	1.737766	0.208584	16	42.07957	2.94E-21
6-OH-BDE-47	8	4.806187	0.055755	16	73.56653	7.56E-29
PBDE - 19	8	0.058935	0.811707	16	3.59287	0.005474
PBDE - 49	8	0.716353	0.411577	16	2.323843	0.050173
PBDE - 190	8	0.186433	0.672478	16	3.685058	0.004658

CHAPTER FOUR

Discussion and Conclusion

Discussion

Cell viability is very basic and, many times, the first indictation of cytotoxicity in *in vitro* toxicology. It is an indication of the toxic insult that a xenobiotic can cause to the cells. Oxidative stress is an early time point in studying cytotoxicity and leads to various cellular malfunctions depending on its intensity. The effects of oxidative stress may be counteracted early on in the cells' life cycle given their defensive mechanisms that help remediation. Apoptosis is one of the several downstream effects that oxidative stress can lead to. This study has thus tried to model the overall cytotoxic influence of PBDEs at an early and a late endpoint in the process of cytotoxicity.

The statistics in Table 2 describe characteristics of the developed QSAR models (equations 2, 3, and 4). These statistics can broadly be classified into *goodness of fit* and *goodness of prediction* criterion. The coefficient of determination, r^2, is the proportion of variability that is accounted for by the model. It is a measure of *goodness of fit* and informs how well the future outcomes are likely to be predicted by the model. The r^2 adjusted (adj) is a modification of r^2 and adjusts it for the varying number of independent variables. It penalizes the model equations containing too many terms to justify their quality of fit. In other words, it checks the models for too many descriptors that

compromise their goodness of fit. The closer the r^2 (adj) value is to r^2, the better is the predictabilty of the model. Friedman lack of fit (LOF) is another measure of the *goodness of fit* for the equations. It scales the mean-squared error with a penalty factor based on the complexity of the model in order to reduce the risk of over fitting. The lower the Friedman lack-of-fit score, the lower are the chances of getting an over fitted model (Todeschini and Consonni, 2000).

Root mean squared error (RMSE) and r^2 predicted (pred) are measures of *goodness of prediction* for the models. RMSE gives a measure of the difference between values predicted by an estimator and the values actually observed for the endpoint being modeled. r^2(pred) works the same way as Predicted Residual Sum of Squares (PRESS) and is an internal validation method. It is the sum of squared differences between the experimental and the predicted values in an internal validation process. Between the *goodness of fit* and the *goodness of prediction* criterion, significance of regression (SOR) is used to determine whether or not the regression is statistically significant (Todeschini and Consonni, 2000).

Control Variability

Figures 6, 7, 8, 11, 12, 13, 16, 17, and 18 represent results from the in vitro experiments. Although the acceptable variation in control and solvent control is variable in different assay systems, a variation of 10-20% in the two responses is considered to be acceptable in in vitro assays (Rand, 1995,). This implies that there should be atleast 80-90% survival for acceptable results from in vitro studies (Brusick, 1987, Landis et al., 1993).

Cell Viability

Cell viability was assessed by exposing Hep G2 cells to the toxic chemicals for 72 hours. PBDE -28, -47, and -99 showed a significant increase in cell toxicity in Hep G2 cells in a dose dependent manner. It is hypothesized that lower brominated PBDE congeners, in solution with culturing media diffused through the cell membranes easily and hampered cellular life processes. It was observed that tri-brominated, tetra- brominated, and pentabrominated PBDEs hampered cell viability more readily than the higher brominated congeners like PBDE-153. Bromine constitutes 50% to 85% of the molecular weight of a PBDE compound (Tittlemier et al., 2002). For instance, PBDE -28 molecule weighs 407 amu out of which bromine counts for 240 amu, i.e., more than 50% of the molecular weight. Bromine atoms are responsible for the fire suppression function of the flame retardants. Higher bromine substitution makes the PBDE structure bulkier. This could be a reason that cells elicited a relatively greater toxic response upon being exposed to lower brominated PBDE congeners. There is considerable research done with PBDE-47 to examine its cytotoxicity. Hu et al., (2009), used the MTT assay to assess the effect of PBDE-47 on Hep G2 cells in a 72-hour study. They observed that the chemical had significant toxic influence from a nominal concentration of 5mg/l to 50 mg/l, dose dependently. Similarly, He et al., (2008), used primary rat neurons for a 24 hour study with PBDE-47 and observed a significant percentage LDH leakage at 20 mg/l dosage. He et al., (2008) tested the cell viability and percentage increase in LDH leakage in human neuroblastoma cell line when exposed to PBDE-47. They observed significant

reduction in both the endpoints measured when dosed at a nominal concentration of 10 mg/l. In another study conducted by Yan et al., (2010), with Jurkat cells, their cell viability was tested upon PBDE-47 exposure with significant reponses from 5 to 50 mg/l nominal concentration in a dose dependent manner. These studies illustrate that the tetrabrominated PBDE congener has been widely studied and has been observed to have significant cytotoxic influences on different kinds of cells. These observations are consistent with the results of the current study. Tetrabrominated congener induced significant oxidative stress (Figures 11 and 12) and cell viability (Figures 6 and 7) in Hep G2 cells.

In the current study, hepta and deca brominated congeners, PBDE -183 and -209, elicited a statistically significant response to the cell viability assay. These congeners were suspected to undergo debromination in solution into octa, penta and other lower brominated PBDE congeners. There are some suggested mechanisms of debromination and consequent cytotoxic effects of these chemicals. Photolytic debromination upon light exposure was speculated as one of the possible mechanisms of debromination by Soderstrom et al., (2004). Another theory regarding debromination was proposed by He et al., (2006), that microbial bacteria could be responsible for anaerobic degradation of bigger molecules belonging to the PBDE family into smaller more toxic congeners. Hu et al., (2007), used MTT assay to assess the effect of PBDE-209 on Hep G2 cells in a 72-hour study. They observed significant reduction in cell viability in a dose-dependent manner. In a similar study conducted by Chen et al., (2009), PBDE-209 gave a significant toxic response upon exposure to MTT assay with primary

cultured neonatal rat hippocampal neurons. Looking at the above studies and the similarity in results observed with the decabrominated PBDE congener (Figures 6 and 11), we can hypothesize that BDE-209 breaks down into lower, more toxic congeners in solution and induces cytotoxicity despite being a bulky congener.

The hydroxylated PBDE congeners were found to be significantly more toxic than the parent congeners, predominantly 6-OH-BDE-47 (Figures 7, 12, and 17). It is being hypothesized that the hydroxy group at the ortho position with relation to the ether linkage in 6-OH-BDE-47 played a pivotal role in intramolecular hydrogen bonding between the hydroxy group and a highly electronegative oxygen atom of the ether linkage. The study is assuming that this added to the hydrophobicity of the molecule and enhanced its ability to exert a toxic effect on the cells (Ghose et al., 1987). This theory regarding 6-OH-BDE-47 toxicity applies to all the endpoints studied and not just cell viability. 6-OH-BDE-47 showed significant toxic influences for almost all the nominal concentrations for every endpoint studied and it is hypothesized that this can be attributed to the above mentioned intramolecular hydrogen bonding. Similar results were obtained in a study done by An et al., (2010). They used the MTT assay and flow cytometry to study respectively the anti–proliferative effect and apoptosis caused by 6-OH-BDE-47 on cultured Hep G2 cells. There was a significant decrease in the cells' ability to proliferate upon being exposed to the chemical and a considerable increase in the rate of apoptosis in the cells. A dose dependent increase in the DCF fluorescence signal was also observed when DCFH-DA was used to study the intracellular ROS production. This is consistent with the findings of the

current study where cell viability (Figure 7), oxidative stress (Figure 12) and apoptosis (Figure 17) experiments gave similar results.

According to equation 2, VSA_AtomicAreas and VSA_PartialCharge are two important descriptors that characterize the cytotoxic influence of PBDEs on Hep G2 cells. Van der Waals surface area (VSA) variants, VSA_AtomicAreas and VSA_PartialCharge are geometric descriptors that characterize cell viability or toxicity. They represent each atom's contribution towards the surface area of the molecule. This has relevance with respect to the theory mentioned earlier that molecules with less bromines, hence smaller structures and less surface area cause more toxicity since it is easier for them to penetrate through the cell membrane and bind to receptors. Degree of bromination makes a difference again because bromine atoms are large and account for more than 50% of the molecular weight for any PBDE molecule (Tittlemier et al., 2002).

VSA_PartialCharge and VSA_AtomicAreas are two dimensional molecular descriptors that belong to the van der Waals surface area family of descriptors. VSA_PartialCharge first calculates the partial charge on each atom of the molecule by Gasteiger's method and further divides the molecular surface area according to an individual atom's partial charge. VSA_AtomicAreas is the atomic contribution of each individual atom towards the total surface area of the molecule. The surface area contribution of any atom in a molecule is the area of that atom not part of any other atom. Assuming the shape of each atom to be a sphere and its radius to be the van der Waal's radius, following mathematical

method section can help calculate the van der Waal's surface area of each atom (Labute, 2011).

Two atoms A and B in a molecule with van der Waal's radius a and b respectively and their centres d units apart are considered. The van der Waal's surface area of the atom A not within atom B can be calculated by the following formula:

$$V_A = \begin{cases} 4\pi a^2 - \pi a d^{-1} [b^2 - (a-d)^2], & \text{if } |a-b| < d < |a+b| \\ 4\pi a^2 & \text{otherwise} \end{cases} \quad \text{(Labute, 2011)} \qquad (5)$$

The atomic surface areas calculated by the above formula can be summed up to find the van der Waal's surface area of the molecule. The above calculation can be generalized for more than two atoms with the assumption that one atom overlapping more than one atoms when neglected would cause a negligible error. An atom A with radius a in contact with B_i more atoms, each with a radius b_i, the centres d_i apart would have the following van der Waal's surface area:

$$V_A = 4\pi a^2 - \pi a \sum^{n}_{i=1} [b_i^2 - (a-d_i)^2] / d_i \, \delta (|a-b_i| < d_i < |a+b_i|) \qquad (6)$$

where δ stands for 1 if the condition following is staisfied and 0 if it is not (Labute, 2011). The above is the method that Discovery Studio used to calculate the approximate values for the VSA_AtomicAreas descriptor for every atom of every PBDE congener used in this study. This mathematical value is shown in Appendix 1 under VSA_AtomicAreas. They represent the calculated values for the descriptor.

Gasteiger Charges is the third descriptor besides VSA_AtomicAreas and VSA_PartialCharge used to characterize the PBDE cytotoxicity in Hep G2 cells. Gasteiger charges is named after scientist Johann Gasteiger who postulated a method for calculating the partial charge on each atom of a molecule. According to his work published in 1979, elecronegativity is one important characteristic of every atom. The topology of a molecule is of prime importance in this method of calculation with considerable weight given to the atomic connectivities. Working at an orbital level, the partial equalization of the electronegativity is obtained through an iterative process of treating the electronegativity. This procedure helps obtain good correlations of the atomic charges with acidity constants and core electron binding energies. Once the atomic charge values have been laid down, it enables prediction of experimental data (Gasteiger and Marsili, 1979).

Gasteiger charges are partial atomic charges, the difference between the orbital charge density of an atom in its unexcited state and when it is in a molecular environment (Gasteiger et al., 1979). The electron affinity as well as the ionization potential of an atom contribute to the partial atomic charge or the electronegativity along with the influence of those from the neighbouring atoms. Gastieger et al. defined this method for partial atomic charge calculation (1980). The PBDE molecule contains 12 carbons each of which is sp^2 hybridized. The two benzene rings have a delocalized pi bond and each of them form a conjugated pi system. The susbstituted bromine atoms have 3 lone pairs of electrons and one singly occupied orbital that forms a σ bond with one of the carbon sp^2 hybrid orbitals. So, the bromine atom has more lone pairs of electrons

than the sigma bonded orbitals. The lone pairs of electrons and pi bonds are strong indicators of valence state electronegativity (Hall et al., 2007). They are located further away from the atomic core as compared the sigma bonded orbitals which means there is lesser shielding effect on them from the nucleus giving rise to higher electronegativity. This can be explained by the fact that the pi and lone pair electron density does not lie along the bond axis. The electrons in the sigma bonded orbitals lie along the bond axis and hence tend to counter the effect of nuclear protons. Thus the atomic core has influence on the sigma bonded electrons much more than that on the pi bonded electrons (Hall et al., 2007). The eletrotopological (E-state) index theory published by Kier and Hall encompasses the above facts. These facts are relevant in the current study. It was observed that the cell toxicity is reduced (equation 2) for a molecule with more bromines substituted or greater atomic electronegativity or higher range gasteiger charge numbers. The higher brominated PBDE congeners with higher electronegativity do not have that significant of an effect on cell viability as compared the lower ones since the higher eletronegativity attribute reduces their effect on cell toxicity. Similarly, 3-OH-BDE-47 and 5-OH-BDE-47 (at lower nominal concentrations) do not have significant toxic effect on the cells since they contain a hydroxy group with a highly electronegative oxygen atom. The high partial atomic charges given the high electronegativity of the substituted atoms influence their affect on cell viability negatively (equation 2).

Oxidative Stress

The oxidative stress endpoint was measured by exposing the PBDE treated cells to the fluorophore DCFH-DA. The DCFH-DA is then hydrolyzed in the cell into highly fluorescent DCF. These fluorescence signals were used to measure oxidative stress for different treatments. Oxidative stress can be a very early toxic endpoint that represents one of the first toxic insults to a cell following exposure to a xenobiotic.

Figures 11 and 12 illustrate the fact that PBDE-47 produces a significant oxidative stress response in Hep G2 cells. As high as 90% oxidative stress increase (when compared to controls) was observed when these cells were subjected to PBDE-47 for 24-hour exposure time. There are a number of previous studies that have observed results similar to the current study. *In vitro* studies by Hu et al., with Hep G2 cells for 72-hour exposure (2009), He et al., with primary rat hippocampal neurons for a 24-hour exposure (2008), He et al., with human neuroblastoma cells for 24-hour exposure time (2008) and Yan et. al., with Jurkat cells for 24-hour exposure time (2010) had similar observations with PBDE-47.

Genetic function approximation determined ALogP_AtomScore and Gasteiger charges as the descriptors used to characterize oxidative stress caused by PBDEs (equation 3). ALogP_AtomScore depicts a hydrophobicity variant as an informative descriptor for PBDEs, which illustrates the chemicals' tendency to be absorbed by fat tissues. AlogP is the hydrophobicity of the chemical under study calculated by an atom based method postulated by Ghose and Crippen (1986). The method uses

hydrophobic atomic constants a_k for estimating individual atomic lipophilicity contributions towards that of the whole molecule (Todeschini and Consonni, 2000). The method was defined by the following model:

$$\text{ALog } P = \sum_k a_k . \text{ N}_k \quad (7)$$

where N_k is the number of atoms of type k in the molecule. The hydrophobic atomic constants (a_k) calculations consider the neighbouring atoms for calculation. The above formula is based on the assumption that a_k or atomic hydrophobicity is an additive property since it is scalar. The different kinds of atoms were broadly categorized into hydrogen, carbon, and hereroatoms. Carbon atoms were classified by their hybridization state and by the atoms bonded to them, whether carbon or heteroatoms. Halogen and hydrogen atoms were classified on the basis of the oxidation and hybrization states of the carbon that they were bonded to. Consideration was also given to the heteroatom bonded to the α-position in the carbon chain of the organic molecule when calculating the hydrophobic atomic constants (Todeschini and Consonni, 2000). There were improvements made to this method in a later work by Viswanadhan, et al., (1990) where there was a correction modeled for the effect of the neighbouring atoms in the form of electronegativity, van der Waal's radius, and bonding pattern by utilizing 36 adjustable parameters. The regression between the observed and calculated values for 893 compounds gave a correlation coefficient of 0.909 and a RMS error value of 0.542. Hence, ALogP_AtomScore descriptor enumerates each atom's contribution to the hydrophobicity of the molecule.

Oxidative stress is directly and additively dependent on the hydrophobicity (ALogP_AtomScore) of a chemical (equation 3). Table 6 illustrates that PBDE -183 has a very high hydrophobicity value (Braekevelt et al., 2003). This characteristic of PBDE -183 is a reasonable theoretical response as to its significant oxidative stress response (only at low nominal concentrations) as shown in Figure 11. Similarly, high Log K_{ow} values for PBDEs -99, -100, and -153 (Table 6 and Figure 11) make them more likely to be taken up easily through the cell membrane, bind to receptors and elicit an oxidative stress response as an immediate biomarker of toxicity. The cell membrane has a phospholipid bilayer that selectively allows only hydrophobic substances to pass through. So compounds with high hydrophobicity values are more likely to diffuse through the membrane.

Table 6. Log K_{ow} values for specific PBDE congeners (Braekevelt et al., 2003)

Chemical	Log K_{ow}
PBDE-28	5.94 ± 0.15
PBDE-47	6.81 ± 0.08
PBDE-99	7.32 ± 0.14
PBDE-100	7.24 ± 0.16
PBDE-153	7.90 ± 0.14
PBDE-183	8.27 ± 0.26

PBDEs -153, -209, -190, and 6-OH-BDE-47 show a gradual increase in percentage oxidative stress in a dose dependent manner. These compounds have a greater partial atomic charge in terms of electronegativity since they have higher bromine substitution (refer to cell viability discussion on Gasteiger charges). Hence, the greater positive contribution of the Gasteiger charges descriptor for these compounds adds to log oxidative stress (equation 3). This implies that bulkier congeners had a greater oxidative stress response in relation to their Gasteiger charges as illustrated by the results on Figures 11 and 12.

Apoptosis

Apoptosis is a later endpoint in the cytotoxicity process. It is sometimes the culmination of the toxic influences of a xenobiotic on the cells. PBDE -100, -47, and -183 showed a significant apoptotic effect on the treated cells. PBDE -100 is a penta brominated congener, one of the most toxic as observed by some studies (He et al., 2006). A significant apoptotic response was observed at almost all the nominal concentrations of PBDE-100. This can also be attributed to its high Log K_{ow} value (Table 3), ALogP_MR being a descriptor that characterizes apoptosis (equation 4). PBDE -47 and -183 produced a significant response at a 10 mg/l nominal concentration when tested for apoptosis (Figure 16). Results similar to the ones in the current study were reported in two other studies with the tetra brominated congener. Yan et al., (2010) dosed Jurkat cells with PBDE-47 in a 48-hour apoptosis study and got a significant increase in percentage apoptosis at 10 mg/l nominal concentration. In a similar study conducted by He et al., (2008), human neuroblastoma cells were treated with PBDE-47 in a 24-

hour study and a significant 8% increase in percentage of apoptotic cell was observed.

QSAR equation for cell apoptosis prediction (equation 4) has ALogP_AtomMRScore, Kappa 3, and VSA_PartialCharge descriptors that characterize the apoptotic trends on cells exposed to PBDEs. ALogP_AtomMRScore is a measure of an individual atom's contribution to the molar refractivity of the compound. Molar refractivity (MR) is defined in terms of polarizability as follows:

$$MR = 4\pi N \alpha/3 \quad \text{(Crippen and Ghose, 1986)} \qquad (8)$$

where N is the Avogadro's number (signifies a mole of substance) and α is the polarizability. Clearly, the molar refractivity (MR) of a substance is a direct function of its polarizability (α). Also, it can be assessed from electrostatics that for a spherical molecule $\alpha = r^3$, where r stands for the radius of a molecule, assuming the molecule to be spherical (Crippen and Ghose, 1986). Substituting this conversion to equation 8 above, it can be said that MR is the same as volume ($4\pi r^3/3$) of spherical molecules in 1 mole of the substance. Theoretically speaking, molecular volume is comprised of each individual atom's volume added together. But that would be true only if we ignore the influence of the atomic bonds' polarity in a molecule and the overlap of the electron clouds of the atoms in coming together to form the molecule (Crippen and Ghose, 1986).

A very similar least square regression method was applied to estimate MR as ALogP (refer to discussion on oxidative stress). It is calculated by the following formula:

$$MR = \sum_k b_k . \ N_k \qquad (9)$$

where b_k is the MR for an atom type and N_k is the number of atoms of type k in the molecule, b_k assumed to be a scalar and additive. The atomic molar refractivities were obtained from densities, refractive indices, atomic weights (Crippen and Ghose 1986), considerations also being given to the temperature and pressure. There was a correction added to the above summation formula (equation 9) to account for the effect of the neighbouring atoms in a later work by Viswanadhan et al., (1990). This effect was modeled in the form of 21 adjustable parameters and the van der Waals radius. Regression was performed on the training set of 547 compounds to give a correlation coefficient of 0.997 and a RMS error of 1.014 between predicted and modeled values Viswanadhan et al., (1990).

Molar refractivity is a measure of the dispersive interaction or polarizability of a substance (Viswanadhan et al., 1990) and is important as a steric descriptor (Nendza, 1998). The polarizability descriptor encompasses the dual nature of a compound, that of the steric bulk and of the changes in the electron distribution in the presence of an electric field. This may lead to the formation of induced atomic diploes in the presence of another local or foreign electric field (Nendza, 1998). Polarizability is directly related to the atomic volume as discussed above under equation 8. The greater the polar parts in a molecule , greater is the MR value for that compound (given the condition of formation of atomic diploles). Molar refractivity as a steric property is responsible for solvation energies of a compound in different solvents, hence it has a role to play in causing hydrophobicity (Nendza, 1998). That could be a possible reason that MR has been

linked with ALogP (atomic level hydrophobicity) in discovery studio. 5-OH-BDE-47 (only at high nominal concentrations), 6-OH-BDE-47 (high hydrophobicity due to intramolecular hydrogen bonding), PBDE-47, PBDE-100, and PBDE-153 produce significant increase in percentage caspase-3 activity (Figure 16) probably because they are more polar as compared the other congeners. The ALogP_AtomMRScore is thus the atomic contribution to the total value of ALogP_MR, the molar refractivity calculated by the atomic method defined by Crippen and Ghose.

Topological indices (TIs) are completely independent of the three dimensional aspect of a chemical structure and use just the 2-D topology of a molecule. These are basically size indices that deal with either one or more structural attributes of a molecule, like shape, symmetry, size, aromaticity, cyclicity, degree of branching, etc. TIs are broadly classified under topostructural indices and topochemical indices. The former deals with the adjacency and distance of atoms in molecular structures, whereas the latter is about characterizing or quantifying topological and chemical information like chemical identity and hybridisation (Todeschini and Consonni, 2000). Kappa indices, in particular are considered dependable for predicting absorption, distribution, metabolism, and excretion related endpoints (Bruce et al., 2008).

Kappa-3 is topostructural index. These descriptors are derived by representing each molecule with a graph excluding the hydrogen atoms called hydrogen suppressed molecule. Atoms are represented as the vertices of the molecular graph and bonds by the edges. They are, in effect, numerical indices of

molecular topology derived by mathematical methods from the molecular structural graphs as described above.

$$^{3}\mathrm{K} = 4.\ ^{3}P_{max}.\ ^{3}P_{min}/\ (^{3}P)^{2}$$

$$= \begin{cases} (A\text{-}3).(A\text{-}2)^{2}/\ (^{3}P)^{2} \text{ for even } A \\ (A\text{-}1).(A\text{-}3)^{2}/(^{3}P)^{2} \text{ for odd } A \end{cases} \text{ (Todeschini and Consonni, 2000)} \qquad (10)$$

where ^{m}P is the number of paths in the hydrogen depleted molecular structure with length m (m=1,2,3) and A is the number of non hydrogen atoms in the molecule.

The topological indices (TI) are divided into three generations depending on their nature. Kappa 3 are second generation third order TI since they are real numbers based on integer graph properties (Estrada and Uriate, 2001). It basically encodes information about the centrality of branching in a molecule. A higher number implies that molecular branching does not exist in the molecular graph or that it is located towards the extreme ends of the graph (Todeschini and Consonni, 2000). The calculated numerical values for the Kappa-3 topological indices have been shown on the Appendix, Table A.1. It clearly shows that the Kappa 3 values for all the PBDE molecules are quite close,which means that there is not a considerable variation in the centrality of branching for the PBDE structures. The number is low for PBDE-209 and PBDE-19 (3.2 and 3.0 respectively) since they are symmetrical structurally and have basically no branching on the fundamental PBDE structure. The value is a bit higher for the other congeners but very close (3.2-3.5) given the unifomity in the dual benzene

ring structure, limited branching and almost uniform atom substitution on the two ether linked aromatic rings part of the fundamental PBDE structure.

VSA_PartialCharge helps characterize the apoptosis caused by PBDEs other than ALogP_AtomMRScore and Kappa-3. The surface area contribution of each individual atom that adds towards the total surface area of the molecule plays a role in characterizing the apoptosis. These atomic surface areas are calculated based on partial atomic charges (refer to discussion under cell viability).

QSAR models designed through this study are represented by equations 2, 3, and 4 are statistically sound and reliable. This is evident from their statistical parameters for the equations listed on Table 2. They were able to predict reliably for the test chemicals, hence were successfully externally validated. There is considerable amount of mechanistic interpretation associated with the cell viability and the oxidative stress QSARs, where the experimental results too can be reasonably explained in terms of the respective descriptors and vice-versa. The apoptosis QSAR, on the contrary, needs more work in terms of improving its mechanistic interpretation.

Conclusions

Tri, tetra, penta, hepta, and deca-brominated PBDE congeners (PBDE -28, -47, -99, -183, and -209) elicited significant toxic responses when tested for cell viability with Hep G2 cells. Van der Waal's surface area and Gastieger charges are the important properties that characterize cell viability. Tetra, hexa, and deca-brominated PBDE congeners (PBDE -47, -153, -209) produced a significant dose

dependent oxidative stress response in Hep G2 cells. Hepta (PBDE-183) was significant at low dosage, whereas tri and penta brominated were found to be significant at only high nominal concentrations. Hydrophobicity and Gastieger charges were important descriptors for characterizing oxidative stress. A penta-brominated congener (PBDE-100) was found to induce significant increases in the rate of apoptosis in a dose-dependent manner. Molar refractivity, Kappa-3, and VSA_PartialCharge were found to be the most appropriate descriptors to characterize this response.

Cell viability, oxidative stress, and apoptosis responses for Hep G2 cells exposed to PBDEs were successfully modeled with an r^2 of 0.9733, 0.922, and 0.9393 respectively (Table 2, Figures 9, 14, and 19). These models, when externally validated, were able to succesfully predict the activities for the test chemicals with r^2 values of 0.827, 0.905, and 0.812 (Figures 10, 15, and 20) respectively. These prediction models can be further improved by expanding the chemical library. More training set data would improve the quality, reliability, and statistical robustness of the models. If there are more fire retardants in the training set, the designed QSARs may be taken to the next level by generalizing the equations for all the fire retardants. Similarly, other important toxic endpoints for PBDE exposures can be modeled for prediction.

The developed and validated QSAR models need to have their applicability domain (AD) defined before they can be used for prediction. Applicability domain for a QSAR model may be defined as "the response and chemical structure space in which the model makes predictions with reliability" (ECVAM Workshop 52,

2005). If the descriptors used in QSAR models are non- discrete or continuous, AD can be defined in terms of the model descriptor space that the training set data lie in. This is because interpolated data are considered more reliable than extrapolated data (ECVAM Workshop 52, 2005). The training set of the current study has chemicals that cover a range of parent PBDE chemicals, identical in their structure and physico-chemical properties and/or their modes of action (assumed uniform if otherwise). It also includes hydroxylated congeners of the parent compounds. The applicability domain of the three developed QSARs thus can be said to include parent PBDEs and their hydroxylated congeners. The test set chemicals must lie in the above stated applicability domain. This research can be taken to the next level and improved by using a more systematic and scientific method for finding the AD for the QSARs generated.

APPENDIX

Calculated Values for Descriptors used in QSAR Equations to Predict the Specific Toxic Endpoints for PBDEs

Table A.1. Calculated values for descriptors used in QSAR equations

Chemical	ALogP_AtomMR Score	ALogP_Atom Score	Gasteiger_Charges	VSA_Atomic Areas	VSA_PartialCharge	Kappa_3
PBDE-28	8.2065	0.8995	-4.79e-002	42.496		3.49519
	3.7593	0.1539	4.94e-002	4.365		
	3.4491	-0.3251	-3.11e-002	9.564		
	3.7593	0.1539	1.88e-002	4.365		
	8.2065	0.8995	-5.08e-002	42.496		
	3.4491	-0.3251	-4.53e-002	9.564		
	3.4491	-0.3251	-2.9e-002	9.564	8.689	
	3.7593	0.1539	9.62e-002	7.867	0	
	1.3502	3.24e-002	-0.3093	8.689	0	
	3.7593	0.1539	8.21e-002	7.867	0	
	3.4491	-0.3251	-3.02e-002	9.564	0	
	3.4491	-0.3251	-4.54e-002	9.564	84.992	
	3.7593	0.1539	1.76e-002	4.365	109.444	
	8.2065	0.8995	-5.09e-002	42.496	13.097	
	3.4491	-0.3251	-4.54e-002	9.564	69.337	
	3.4491	-0.3251	-3.02e-002	9.564	0	
	0.8939	0.6301	6.47e-002	7.657	0	
	0.8939	0.6301	6.35e-002	7.657	0	
	0.8939	0.6301	6.51e-002	7.657	0	
	0.8939	0.6301	6.5e-002	7.657	0	
	0.8939	0.6301	6.35e-002	7.657		
	0.8939	0.6301	6.35e-002	7.657		
	0.8939	0.6301	6.61e-0	7.657		

Table A.1 continued.

Chemical	ALogP_AtomMR Score	ALogP_Atom Score	Gasteiger_Charges	VSA_Atomic Areas	VSA_PartialCharge	Kappa_3
PBDE-47	3.4491	-0.3251	-4.53e-002	9.564	8.689 0 0 0 0 84.992 142.376 17.462 61.679 0 0 0 0 0	3.48444
	3.4491	-0.3251	-2.9e-002	9.564		
	3.7593	0.1539	9.63e-002	7.867		
	3.7593	0.1539	4.94e-002	4.365		
	3.4491	-0.3251	-3.11e-002	9.564		
	3.7593	0.1539	1.88e-002	4.365		
	8.2065	0.8995	-5.08e-002	42.496		
	8.2065	0.8995	-4.79e-002	42.496		
	1.3502	3.24e-002	-0.3081	8.689		
	3.7593	0.1539	9.63e-002	7.867		
	3.7593	0.1539	4.94e-002	4.365		
	3.4491	-0.3251	-3.11e-002	9.564		
	3.7593	0.1539	1.88e-002	4.365		
	3.4491	-0.3251	-4.53e-002	9.564		
	3.4491	-0.3251	-2.9e-002	9.564		
	8.2065	0.8995	-5.08e-002	42.496		
	8.2065	0.8995	-4.79e-002	42.496		
	0.8939	0.6301	6.35e-002	7.657		
	0.8939	0.6301	6.51e-002	7.657		
	0.8939	0.6301	6.47e-002	7.657		
	0.8939	0.6301	6.47e-002	7.657		
	0.8939	0.6301	6.35e-002	7.657		
	0.8939	0.6301	6.58000	7.657		

Table A.1-continued.

Chemical	ALogP_AtomMR Score	ALogP_Atom Score	Gasteiger_Charges	VSA_Atomic Areas	VSA_PartialCharge	Kappa_3
PBDE-99	3.4491			9.564		3.52617
	3.4491	-0.3251	-4.53e-002	9.564		
	3.7593	-0.3251	-2.9e-002	7.867		
	3.7593	0.1539	9.63e-002	4.365		
	3.4491	0.1539	4.94e-002	9.564		
	3.7593	-0.3251	-3.11e-002	4.365		
	8.2065	0.1539	1.88e-002	42.496	8.689	
	8.2065	0.8995	-5.08e-002	42.496	0	
	1.3502	0.8995	-4.79e-002	8.689	0	
	3.7593	3.24e-002	-0.308	7.867	0	
	3.4491	0.1539	9.74e-002	9.564	0	
	3.7593	-0.3251	-1.47e-002	4.365	42.496	
	3.7593	0.1539	3.43e-002	4.365	217.804	
	3.4491	0.1539	3.3e-002	9.564	21.828	
	3.7593	-0.3251	-2.99e-002	4.365	54.022	
	8.2065	0.1539	4.95e-002	42.496	0	
	8.2065	0.8995	-4.79e-002	42.496	0	
	8.2065	0.8995	-4.96e-002	42.496	0	
	0.8939	0.8995	-4.95e-002	7.657	0	
	0.8939	0.6301	6.35e-002	7.657	0	
	0.8939	0.6301	6.51e-002	7.657		
	0.8939	0.6301	6.47e-002	7.657		
	0.8939	0.6301	6.63e-002	7.657		
		0.6301	6.54e-00			

Table A.1 continued.

Chemical	ALogP_AtomMR Score	ALogP_Atom Score	Gasteiger_Charges	VSA_Atomic Areas	VSA_PartialCharge	Kappa_3
	3.4491	-0.3251	-4.53e-002	9.564		
	3.4491	-0.3251	-2.9e-002	9.564		
	3.7593	0.1539	9.63e-002	7.867		
	3.7593	0.1539	4.94e-002	4.365		
	3.4491	-0.3251	-3.11e-002	9.564		
	3.7593	0.1539	1.88e-002	4.365		
	8.2065	0.8995	-5.08e-002	42.496		
	8.2065	0.8995	-4.79e-002	42.496		
	1.3502	3.24e-002	-0.3069	8.689		
	3.7593	0.1539	0.1105	7.867	8.689	
PBDE-100	3.7593	0.1539	5.06e-002	4.365	0	
	3.4491	-0.3251	-3.1e-002	9.564	0	3.52617
	3.7593	0.1539	1.99e-002	4.365	0	
	3.4491	-0.3251	-3.1e-002	9.564	0	
	3.7593	0.1539	5.06e-002	4.365	84.992	
	8.2065	0.8995	-4.79e-002	42.496	175.308	
	8.2065	0.8995	-5.08e-002	42.496	13.097	
	8.2065	0.8995	-4.79e-002	42.496	54.886	
	0.8939	0.6301	6.35e-002	7.657	7.867	
	0.8939	0.6301	6.51e-002	7.657	0	
	0.8939	0.6301	6.47e-002	7.657	0	
	0.8939	0.6301	6.47e-002	7.657	0	
	0.8939	0.6301	6.55e-002	7.657	0	

Table A.1 continued.

Chemical	ALogP_AtomMR Score	ALogP_Atom Score	Gasteiger_Charges	VSA_Atomic Areas	VSA_PartialCharge	Kappa_3
	3.4491	-0.3251	-1.47e-002	9.564		
	3.7593	0.1539	9.74e-002	7.867		
	3.7593	0.1539	4.95e-002	4.365		
	3.4491	-0.3251	-2.99e-002	9.564		
	3.7593	0.1539	3.3e-002	4.365		
	3.7593	0.1539	3.43e-002	4.365		
	8.2065	0.8995	-4.95e-002	42.496		
	8.2065	0.8995	-4.96e-002	42.496		
	8.2065	0.8995	-4.79e-002	42.496	8.689	
	1.3502	3.24e-002	-0.308	8.689	0	
	3.7593	0.1539	9.74e-002	7.867	0	
PBDE-153	3.4491	-0.3251	-1.47e-002	9.564	0	3.55555
	3.7593	0.1539	3.43e-002	4.365	0	
	3.7593	0.1539	3.3e-002	4.365	0	
	3.4491	-0.3251	-2.99e-002	9.564	293.232	
	3.7593	0.1539	4.95e-002	4.365	26.194	
	8.2065	0.8995	-4.79e-002	42.496	46.364	
	8.2065	0.8995	-4.96e-002	42.496	0	
	8.2065	0.8995	-4.95e-002	42.496	0	
	0.8939	0.6301	6.63e-002	7.657	0	
	0.8939	0.6301	6.47e-002	7.657	0	
	0.8939	0.6301	6.63e-002	7.657	0	
	0.8939	0.6301	6.55e-00	7.657		

Table A.1 continued.

Chemical	ALogP_AtomMR Score	ALogP_Atom Score	Gasteiger_Charges	VSA_Atomic Areas	VSA_PartialCharge	Kappa_3
	8.2065	0.8995	-4.79e-002	42.496		
	3.7593	0.1539	5.06e-002	4.365		
	3.4491	-0.3251	-2.99e-002	9.564		
	3.7593	0.1539	3.41e-002	4.365		
	8.2065	0.8995	-4.95e-002	42.496		
	3.7593	0.1539	4.86e-002	4.365		
	8.2065	0.8995	-4.83e-002	42.496		
	3.7593	0.1539	6.48e-002	4.365		
	8.2065	0.8995	-4.67e-002	42.496	8.689	
	3.7593	0.1539	0.1116	7.867	0	
PBDE-183	1.3502	3.24e-002	-0.3068	8.689	0	
	3.7593	0.1539	9.75e-002	7.867	0	
	3.7593	0.1539	4.95e-002	4.365	0	3.4425
	8.2065	0.8995	-4.79e-002	42.496	0	
	3.4491	-0.3251	-2.99e-002	9.564	326.164	
	3.7593	0.1539	3.3e-002	4.365	21.828	
	8.2065	0.8995	-4.96e-002	42.496	39.571	
	3.7593	0.1539	3.43e-002	4.365	7.867	
	8.2065	0.8995	-4.95e-002	42.496	0	
	3.4491	-0.3251	-1.47e-002	9.564	0	
	0.8939	0.6301	6.47e-002	7.657	0	
	0.8939	0.6301	6.47e-002	7.657	0	
	0.8939	0.6301	6.73e-002	7.657		

Table A.1 continued.

Chemical	ALogP_AtomMR Score	ALogP_Atom Score	Gasteiger_Charges	VSA_Atomic Areas	VSA_PartialCharge	Kappa_3
	3.7593	0.1539	0.1128	7.867		
	3.7593	0.1539	6.48e-002	4.365		
	3.7593	0.1539	4.97e-002	4.365		
	3.7593	0.1539	4.83e-002	4.365		
	3.7593	0.1539	4.97e-002	4.365		
	3.7593	0.1539	6.48e-002	4.365		
	8.2065	0.8995	-4.66e-002	42.496		
	8.2065	0.8995	-4.82e-002	42.496		
	8.2065	0.8995	-4.83e-002	42.496	8.689	
	8.2065	0.8995	-4.82e-002	42.496	0	
	8.2065	0.8995	-4.66e-002	42.496	0	
	1.3502	3.24e-002	-0.3055	8.689	0	
PBDE-209	3.7593	0.1539	0.1128	7.867	0	
	3.7593	0.1539	6.48e-002	4.365	0	
	3.7593	0.1539	4.97e-002	4.365	424.96	3.25443
	3.7593	0.1539	4.83e-002	4.365	26.194	
	3.7593	0.1539	4.97e-002	4.365	17.462	
	3.7593	0.1539	6.48e-002	4.365	15.734	
	8.2065	0.8995	-4.66e-002	42.496	0	
	8.2065	0.8995	-4.82e-002	42.496	0	
	8.2065	0.8995	-4.83e-002	42.496	0	
	8.2065	0.8995	-4.82e-002	42.496	0	
	8.2065	0.8995	-4.55e-002	42.496		

Table A.1 continued.

Chemical	ALogP_AtomMR Score	ALogP_Atom Score	Gasteiger_Charges	VSA_Atomic Areas	VSA_PartialCharge	Kappa_3
3-OH-BDE-47	3.4491	-0.3251	-4.14e-002	9.564	24.485	3.32179
	3.4491	-0.3251	-2.87e-002	9.564	0	
	3.7593	0.1539	0.1002	7.867	0	
	3.7593	0.1539	9.68e-002	4.365	0	
	3.7593	0.1539	0.209	7.867	0	
	3.7593	0.1539	6.62e-002	4.365	42.496	
	8.2065	0.8995	-4.66e-002	42.496	175.308	
	8.2065	0.8995	-4.37e-002	42.496	8.731	
	1.3502	3.24e-002	-0.308	8.689	54.886	
	3.7593	0.1539	9.63e-002	7.867	7.867	
	3.7593	0.1539	4.94e-002	4.365	0	
	3.4491	-0.3251	-3.11e-002	9.564	7.867	
	3.7593	0.1539	1.87e-002	4.365	0	
	3.4491	-0.3251	-4.53e-002	9.564	0	
	3.4491	-0.3251	-2.9e-002	9.564	42.496	
	8.2065	0.8995	-5.08e-002	42.496	175.308	
	8.2065	0.8995	-4.8e-002	42.496	8.731	
	-999	-0.7941	-1.2873	15.795	54.886	
	0.8939	0.6301	6.36e-002	7.657	7.867	
	0.8939	0.6301	6.51e-002	7.657	0	
	0.8939	0.6301	6.47e-002	7.657	7.867	
	0.8939	0.6301	6.35e-002	7.657	0	
	0.8939	0.6301	6.64000000000003e-002	7.657	0	

Table A.1 continued.

Chemical	ALogP_AtomMR Score	ALogP_Atom Score	Gasteiger_Charges	VSA_Atomic Areas	VSA_PartialCharge	Kappa_3
5-OH-BDE-47	3.7593	0.1539	0.1949	7.867		3.52617
	3.4491	-0.3251	1.86e-002	9.564		
	3.7593	0.1539	0.1002	7.867		
	3.7593	0.1539	4.97e-002	4.365		
	3.4491	-0.3251	-2.71e-002	9.564		
	3.7593	0.1539	6.61e-002	4.365		
	8.2065	0.8995	-4.66e-002	42.496		
	8.2065	0.8995	-4.8e-002	42.496		
	1.3502	3.24e-002	-0.308	8.689	24.485	
	3.7593	0.1539	9.63e-002	7.867	0	
	3.7593	0.1539	4.94e-002	4.365	0	
	3.4491	-0.3251	-3.11e-002	9.564	0	
	3.7593	0.1539	1.87e-002	4.365	0	
	3.4491	-0.3251	-4.53e-002	9.564	42.496	
	3.4491	-0.3251	-2.9e-002	9.564	165.744	
	8.2065	0.8995	-5.08e-002	42.496	22.661	
	8.2065	0.8995	-4.8e-002	42.496	50.52	
	-999	-0.7941	-1.2886	15.795	7.867	
	0.8939	0.6301	6.92e-002	7.657	7.867	
	0.8939	0.6301	6.48e-002	7.657	0	
	0.8939	0.6301	6.47e-002	7.657	0	
	0.8939	0.6301	6.35e-002	7.657	0	
	0.8939	0.6301	6.64000000000003e-002	7.657		

Table A.1 continued.

Chemical	ALogP_AtomMR Score	ALogP_Atom Score	Gasteiger_Charges	VSA_Atomic Areas	VSA_PartialCharge	Kappa_3
6-OH-BDE-47	3.4491	-0.3251	2.5e-003	9.564		
	3.7593	0.1539	0.211	7.867		
	3.7593	0.1539	0.1435	7.867		
	3.7593	0.1539	5.34e-002	4.365		
	3.4491	-0.3251	-3.08e-002	9.564		
	3.7593	0.1539	2.26e-002	4.365		
	8.2065	0.8995	-5.07e-002	42.496		
	8.2065	0.8995	-4.78e-002	42.496		
	1.3502	3.24e-002	-0.304	8.689		
	3.7593	0.1539	9.65e-002	7.867	24.485	
	3.7593	0.1539	4.94e-002	4.365	0	
	3.4491	-0.3251	-3.11e-002	9.564	0	3.52617
	3.7593	0.1539	1.87e-002	4.365	0	
	3.4491	-0.3251	-4.53e-002	9.564	0	
	3.4491	-0.3251	-2.9e-002	9.564	84.992	
	8.2065	0.8995	-5.08e-002	42.496	123.248	
	8.2065	0.8995	-4.8e-002	42.496	22.661	
	-999	-0.7941	-1.2869	15.795	50.52	
	0.8939	0.6301	6.76e-002	7.657	7.867	
	0.8939	0.6301	6.47e-002	7.657	0	
	0.8939	0.6301	6.47e-002	7.657	7.867	
	0.8939	0.6301	6.35e-002	7.657	0	
	0.8939	0.6301	6.63000000000001e-002	7.657	0	

Table A.1 continued.

Chemical	ALogP_AtomMR Score	ALogP_Atom Score	Gasteiger_Charges	VSA_Atomic Areas	VSA_PartialCharge	Kappa_3
	3.4491	-0.3251	-4.53e-002	9.564		
	3.7593	0.1539	4.83e-002	4.365		
	3.7593	0.1539	9.63e-002	7.867		
	1.3502	3.24e-002	-0.3069	8.689		
	3.7593	0.1539	0.1104	7.867		
	3.7593	0.1539	4.94e-002	4.365		
	3.4491	-0.3251	-4.53e-002	9.564		
	3.4491	-0.3251	-5.99e-002	9.564		
	3.4491	-0.3251	-4.53e-002	9.564		
	3.7593	0.1539	4.94e-002	4.365	8.689	
	3.4491	-0.3251	-3.01e-002	9.564	0	
	3.4491	-0.3251	-5.96e-002	9.564	0	3.02972
PBDE-19	3.4491	-0.3251	-6.1e-002	9.564	0	
	8.2065	0.8995	-4.8e-002	42.496	0	
	8.2065	0.8995	-4.79e-002	42.496	28.692	
	0.8939	0.6301	6.35e-002	7.657	165.744	
	0.8939	0.6301	6.23e-002	7.657	13.097	
	0.8939	0.6301	6.35e-002	7.657	61.47	
	0.8939	0.6301	6.5e-002	7.657	7.867	
	0.8939	0.6301	6.23e-002	7.657	0	
	0.8939	0.6301	6.35e-002	7.657	0	
	8.2065	0.8995	-4.79e-002	42.496	0	
	0.8939	0.6301	6.33e-002	7.657	0	

Table A.1 continued.

Chemical	ALogP_AtomMR Score	ALogP_Atom Score	Gasteiger_Charges	VSA_Atomic Areas	VSA_PartialCharge	Kappa_3
PBDE- 49	3.7593	0.1539	1.88e-002	4.365	8.689 0 0 0 0 84.992 142.376 17.462 61.679 0 0 0 0 0	3.48444
	3.4491	-0.3251	-3.11e-002	9.564		
	3.7593	0.1539	4.94e-002	4.365		
	3.7593	0.1539	9.63e-002	7.867		
	1.3502	3.24e-002	-0.308	8.689		
	3.7593	0.1539	9.73e-002	7.867		
	3.4491	-0.3251	-1.59e-002	9.564		
	3.7593	0.1539	2.01e-002	4.365		
	3.4491	-0.3251	-4.67e-002	9.564		
	3.4491	-0.3251	-4.42e-002	9.564		
	3.7593	0.1539	4.84e-002	4.365		
	3.4491	-0.3251	-2.9e-002	9.564		
	3.4491	-0.3251	-4.53e-002	9.564		
	0.8939	0.6301	6.47e-002	7.657		
	8.2065	0.8995	-4.79e-002	42.496		
	8.2065	0.8995	-5.08e-002	42.496		
	0.8939	0.6301	6.35e-002	7.657		
	8.2065	0.8995	-4.8e-002	42.496		
	0.8939	0.6301	6.35e-002	7.657		
	8.2065	0.8995	-5.08e-002	42.496		
	0.8939	0.6301	6.62e-002	7.657		
	0.8939	0.6301	6.34e-002	7.657		
	0.8939	0.6301	6.61e-002	7.657		

Table A.1 continued.

Chemical	ALogP_AtomMR Score	ALogP_Atom Score	Gasteiger_Charges	VSA_Atomic Areas	VSA_PartialCharge	Kappa_3
	3.7593	0.1539	6.49e-002	4.365		
	3.7593	0.1539	4.97e-002	4.365		
	3.7593	0.1539	4.83e-002	4.365		
	3.7593	0.1539	4.97e-002	4.365		
	3.7593	0.1539	6.49e-002	4.365		
	3.7593	0.1539	0.1127	7.867		
	1.3502	3.24e-002	-0.308	8.689		
	3.7593	0.1539	8.33e-002	7.867	8.689	
	3.4491	-0.3251	-3.01e-002	9.564	0	
	3.4491	-0.3251	-4.43e-002	9.564	0	
	3.7593	0.1539	3.18e-002	4.365	0	
PBDE-190	3.7593	0.1539	3.43e-002	4.365	0	3.27662
	3.4491	-0.3251	-1.59e-002	9.564	0	
	8.2065	0.8995	-4.83e-002	42.496	326.164	
	8.2065	0.8995	-4.67e-002	42.496	21.828	
	8.2065	0.8995	-4.95e-002	42.496	39.571	
	8.2065	0.8995	-4.67e-002	42.496	7.867	
	8.2065	0.8995	-4.83e-002	42.496	0	
	8.2065	0.8995	-4.83e-002	42.496	0	
	0.8939	0.6301	6.5e-002	7.657	0	
	0.8939	0.6301	6.35e-002	7.657	0	
	8.2065	0.8995	-4.96e-002	42.496		
	0.8939	0.6301	6.76e-002	7.657		

BIBLIOGRAPHY

An, J., Li, S., Zhong, Y., Wang, Y., Zhen, K., Zhang, X., Wang, Y., Wu, M., Yu, Z., Sheng, G., Fu, J., Huang, Y. 2010. The cytotoxic effects of synthetic 6-hydroxylated and 6-methoxylated polybrominated diphenyl ether 47 (BDE47). *Wiley Interscience*. DOI 10.1002/tox.20582

Banga, I., Lax, K., Szent-Gyorgyi, A. 1933. Uber die Oxydation der Milchs# {227}ure und der fl-Oxybuttersaure durch den Herzmuskel, *Physiol. Chem.* 217: 43-53, 1933.

Barratt, M. D. 1998. Integration of QSAR and in vitro toxicology. *Environmental Health Perspectives* 106, 2 (1998) 459-465.

Bensley, R. R. 1911.Studies on the pancreas of the guinea pig, Am. *J. Anat*., 12**:** 297-388, 1911.

Bensley, R. R. and Bensley, S. H. 1938. Handbook of histological and cytological technique, Univ. of Chicago Press, Chicago, 1938.

Braekevelt, E., Tittlemier, S. A., Tomy, G. T. 2003. Direct measurement of octanol-water partition coefficients of some environmentally relevant brominated diphenyl ether congeners. *Chemosphere* 51 (2003) 563-567.

Bruce, E. D., Autenrieth, R. L., Burghardt, R. C, Donnelly, K. C., McDonald, T. J. 2008. Using quantitative structure-activity relationships (QSAR) to predict toxic endpoints for polycyclic aromatic hydrocarbons (PAH). *Journal of Toxicology and Environmental Health* Part A: 1073-1084

Brusick, David. Principles of Genetic Toxicology, second edition. 1987. New York: Plenum Press

Cathcart, R., Schwiers, E., Ames, B. N. 1983. Detection of picomole levels of hydroperoxides using a fluorescent dichlorofluorescein assay. *Analytical Biochemistry* 134, 111-116.

Chen, J., Liufu, C., Sun, W., Sun, X., Chen, D. 2009. Assessment of the neurotoxic mechanisms of decabrominated diphenyl ether (PBDE-209) in primary cultured neonatal rat hippocampal neurons include alterations in second messenger signaling and oxidative stress. *Toxicological Letters*.

Chen, J., Harner, T., Ding, G., Quan, X., Schramm, K. W., Kettrup, A. @004. Universal predictive models on octanol-air partition coefficients at different temperatures for persistent organic pollutants. *Engironmental Toxicology and Chemistry* 23, 10 (2004) 2309-2317.

Cronin, M. T. D. 2002. The current status and future applicability of quantitative structure-activity relationships in predicting toxicity. *ATLA* 30, Supplement 2, 81-84.

Crippen, G., Ghose, A. K. 1986. Atomic physicochemical parameters for three-dimensional structure-directed quantitative structure-activity relationships I. Partition coefficient as a measure of hydrophobicity .*J. Comp. Chem.* 1986, 7, 565-577.

Dearden, J. C., Cronin, M. T. D., Kaiser, K. L. E. 2009. How not to develop a quantitative structure-activity or structure-property relationship (QSAR/QSPR). *SAR and QSAR in Environmental Research* 20, 3-4 (2009) 241-266.

ECVAM workshop 52. 2005. Current status of methods for defining the applicability domain of (quantitative) structure-activity relationships. *ATLA* 33, 1-19, 2005

Estrada, E., Uriarte, E. 2001. Recent advances on the role of topological indices in drug discovery research. *Current Medicinal Chemistry* 8 (2001) 1573-1588.

Fernie, K. J., Shutt, J. L., Mayne, G., Hoffman, D., Letcher, R. J., Drouillard, K. G., Ritchie, I. J. 2005. Exposure to polybrominated diphenyl ethers (PBDEs): change in thyroid, vitamin A, glutathione homeostasis and oxidative stress in American Keestrels (*Falco sparverius*), *Toxicol. Sci*. 88, 375-383.

Fisher, A. J., Cruz, W. D., Zoog, S. J., Schneider, C. L., Friesen, P. D. 1999. Crystal structure of baculovirus P35: role of a novel reactive site loop in apoptotic caspase inhibition. *Trends Biochem Sci* 22, 388 (1997).

Frimurer, T.M., Bywater, R., Narum, L., Lauritsen, L.N., Brunak, S. 2000. Improving the odds in discriminating drug-like from non drug-like compounds. *Journal of Chem. Inf. Computer Science*. 40, 280-292.

Gasteiger, J. 1988. Empirical methods for the calculation of physicochemical data of organic compounds. *The Physical Property Prediction in Organic Chemistry.* (1988) 119-138.

Gasteiger, J., Marsili, M. 1980. Iterative partial equalization of orbital electronegativity- a rapid access to atomic charges. *Tetrahedron* 36, 3219-3288.

Giordano, G., Kavanagh, T. J. and Costa, L. G. 2009. Mouse cerebellar astrocytes protect cerebellar granule neurons against toxicity of the polybrominated diphenyl ether (PBDE) mixture DE-71. *Neuro Toxicology* 30 (2009) 326-329.

Ghose, A. K.; Crippen G. 1987. Atomic physicochemical parameters for three-dimensional structure-directed quantitative structure-activity relationships. 2. Modeling dispersive and hydrophobic interactions. *J. Chem. Inf. Comput. Sci.* 27:1 (1987) 21-35.

Ghose, A. K., Pritchett, A., Crippen, G. M. 1987. Atomic physicochemical parameters for three dimensional structure directed quantitative structure-activity relationships III: Modeling hydrophobic interactions. *Journal of Computational Chemistry* 9:1 (1987) 80-90.

Gustafsson, K., Björk, M., Burreau, S., Gilek, M., 1999. Bioaccumulation kinetics of brominated flame retardants (polybrominated diphenyl ethers) in blue mussels (Mytilus edulis). *Environ. Toxciol. Chem*. 18, 1218–1224.

Hall, L. H., Kier, L. B., Hall, L. M. 2007. Electrotopological state indices to assess molecular and absorption, distribution, metabolism, excretion, and toxicity properties. *Comprehensive Medicinal Chemistry II* 5 (2007) 555-576.

Hall, L. H., Kier, L. B., Hall, L. M. 2007. Topological quantitative structure-activity relationship applications: Structure information representation in drug discovery. *Comprehensive Medicinal Chemistry II* 4 (2007) 537-574.

Hansch, C., Selassie, C. 2007. Quantitative Structure–Activity Relationship – A Historical Perspective and the Future. In John B. Taylor, David J. Triggle, Eds, *Comprehensive Medicinal Chemistry II,* Elsevier, Oxford, pp 43-63.

Harju, M., Hamers, T, Kamstra, J. H., Sonneveld, E., Boon, J. P. 2007. Quantitative structure-activity relationship modeling on in vitro endocrine effects and metabolic stability involving 26 selected brominated flame retardants. *Environmental Toxicology and Chemistry*, vol. 26, no. 4: 816-826.

Harju, M., Andersson P. L., Haglund P., Tysklind M. 2001. Multivariate physicochemical characterization and quantitative structure-property relationship modeling of Polybrominated diphenyl ethers. *Chemoshpere* 47 (2001) 375-384.

Konemann, H. 1981. Quantitative structure-activity relationships in fish toxicity studies. Part 1: Relationship for 50 industrial chemicals. *Toxicology*, 19:229-238.

Harju, M., Hamers, T., Kamstra, J. H., Sonneveld, E., Boon, J. P., Tysklind, M., Andersson, P. L. 2007. Quantitative structure-activity relationship modeling on in vitro endocrine effects and metabolic stability involving 26 selected brominated flame retardants. *Environmental Toxicology and Chemistry* 26: 4 (2006) 816-826.

He, P., He, W., Wang, A., et al. 2008. PBDE-47-induced oxidative stress, DNA damage and apoptosis in primary cultured rat hippocampal neurons. *Neuro Toxicology 29* (2008) 124-129.

He, J., Robrock, K. B., Alvarex-Cohen, L. 2006. Microbial reductive debromination of Polybrominated diphenyl ethers (PBDEs). *Environmental Science and Technology* 40:16, 4429-4434.

He, W., He, P., Wang, A., Xia, T., Xu, B., Chen, X. 2008. Effects of PBDE-47 on cytotoxicity and genotoxicity in human neuroblastoma cells in vitro. *Mutation Research* 649 (2008) 62-70.

Hine, J., Mookerjee, P.K. 1975. The intrinsic hydrophilic character of organic compounds, correlations in terms of structural contributions. *Journal of Organic Chemistry* 40:3 (1975) 292-298.

Hu, Q., Liang, Y., Yin, H., Peng, X., Fang, K. 2004. Structural interpretation of the topological index. 2. The molecular connectivity index, the kappa index, and the atom type e-state index. *J. chem.. inf. Comput. Sci.* 44 (2004) 1193-1201.

Hu, X., Hu, D., Xu, Y. 2009. Effects of tetrabrominated diphenyl ether and hexabromocyclododecanes in single and complex exposure to hepatoma Hep G2 cells. *Environmental Toxicology and Pharmacology* 27 (2009) 327-337.

Hu, X.-Z., Xu, Y., Hu, D.-C., Hui, Y., Y, F.-X. 2007. Apoptosis induction on human heptaoma cells Hep G2 of decabrominated diphenyl ether (PBDE-209). *Toxicology Letters* 171 (2007) 19-28.

Hui-Ying, X., Jian-Wei, Z., Qing-Sen, Y., Yan-Hua, W., Jian-Ying, Z., Hai-Xiao, J. 2007. QSPR/QSAR models for prediction of the physicochemical properties and biological activity of polybrominated diphenyl ethers. *Chemosphere* 66 (2007) 1998-2010.

Jacobs, M. N. 2004. In silico tools to aid risk assessment of endocrine disrupting chemicals. *Toxicology* 205 (2004) 43-53.

Konneman, H. 1981. Quantitative structure-activity relationships in fish toxicity studies. Part 1: Relationship for 50 industrial chemicals. Toxicology, 19:209-221.

Labute, P. 2011. A widely applicable set of descriptors. *Chemical Computing Group Inc.*

Landis W. G., Hughes, J. S., Lewis, M. A. 1993. Environmental Toxicology and Risk Assessment. STP 1179.

Lasarow, A., Cooperstein, S. J. Studies on the enzymatic basis for the Janus Green B* staining reaction. The Department of Anatomy, Western Reserve University, Cleveland 6, Ohi, 234-241.

Law, R. J., Alaee, M., Allchin, C. R., Boon, J. P., Lebeuf, M., Lepom, P., Stern, G. A. 2003. Levels and trends of polybrominated diphenyl ethers and other brominated flame retardants in wildlife. *EnvironInt* 29:757–770.

Lewis**,** M. R. 1023.The destruction of *Bacillus radicicola* by the connective tissue cells of the chick embryo *in vitro,* Johns Hopkins Hosp. Bull. 34: 223-226**,** 1923.

Lewis**,** W. H., Lewis**,** M. R. 1924. Behavior of cells in tissue cultures, General Cytology, edited by E. V. Cowdry, *Chicago Press, Chicago*, pp. 385-447, 1924.

Li, F., Xie, Q., Li, X., Li, N., Chi, P., Chen, J., Want, Z., Hao, C. 2010. Hormone activit of hydroxylated polybrominated diphenyl ethers on human thyroid receptor- β: In vitro and in silico investigations. *Environmental Health Perspectives* 118: 5 (2010) 602-606.

Liu, Y. 2004. A comparative study on feature selection methods for drug discovery. *Journal of Chem. Inf. Comput. Sci.* 44, 1823-1828.

Liu, Y. 2005. Drug design by machine learning: ensemble learning for QSAR modeling. Proceedings of the fourth International Conference on Machine Learning and Applications.

Madia, F., Giordano, G., Fattori, V., Vitalone, A., Branchi, I., Capone, F., et al. 2004. Differential in vitro neurotoxicity of the flame retardant PBDE-99 and of the PCB Aroclor 1254 in human astrocytoma cells. *Toxicol. Lett*; 154:11-21.

Mannhold, R., van de Waterbeemd, H. 2000. Substructure and whole molecule approaches for calculating log *P*. *Journal of Computer-Aided Molecular Design* 15 (2001) 337-354.

Mao, B., Gozalbes, R., Barbosa, F., Migeon, J., Merrick, S., Kamm, K., Wong, E., Costales, C., Shi, W., Wu, C., Froloff, N. 2006. QSAR modeling of in vitro inhibition of cytochrome P450 3A4. *J. Chem. Inf. Model.* 46, (2006) 2125-2134.

Meeker, J. D., Johnson, P. I., Camann, D., Hauser, R. 2009. Polybrominated diphenyl ether (PBDE) concentration in house dust is related to hormone levels in men. *Science and Total Environment* 407 (2009) 3425-3429.

Mundy, W. R., Freudenrich, T. M., Crofton, K. M., DeVitro, M. J. 2004. Accumulation of PBDE-47 in primary cultures of rat neocortical cells. *Toxicological Sciences* 28:1 (2004) 164-169.

Nendza, M. 1998. Structure-Activity Relationships in Environmental Sciences. Chapman & Hall.

Nicholson DW, Ali A, Thornberry NA, Vaillancourt JP, Ding CK, Gallant M, Gareau Y, Griffin PR, Labelle M, Lazebnik YA, et al. Identification and inhibition of the ICE/CED-3 protease necessary for mammalian apoptosis. *Nature*. 1995 Jul 6; 376(6535):17-8

Papa, E., Kovarich, S., Gramatica, P., 2010. QSAR modeling and prediction of the endocrine-disrupting potencies of brominated flame retardants. *Chem. Res. Toxicology.* 2010, 23, 946-954.

Rand, G. M. 1995. Fundamentals of Aquatic Toxicology: Effects, Environmental Fate, and Risk Assessment. Francis and Taylor.

Reistad, T., Mariussen, E. 2005. Commercial mixture of the brominated flame retardant pentabrominated diphenyl ether (DE-71) induces respiratory burst in human neutrophil granulocytes in vitro. *Toxicol. Sci*. 87, 57-65.

Rogers, D., Hopfinger, A. J. 1994. Application of genetic function approximation to quantitative structure-activity relationships and quantitative structure-property relationships. *J. Chem. Inf. Comput. Sci.* 34 (1994) 854-866.

Samara, F., Gullett, B. K., Harrison, R. O., Chu, A., Clark, G. C. 2009. Determination of relative assay response factors for toxic chlorinated and brominated dioxins/furans using an enzyme immunoassay (EIA) and a chemically-activated luciferase gene expression cell bioassay (CALUX). *Environ Int* 35:588-593.

Schecter, A., Pavuk, M., Pa¨pke, O., Ryan, J.J., Birnbaum, L., Rosen, R., 2003.Polybrominated diphenyl ethers (PBDEs) in US mothers' milk. *Environ. HealthPerspect.* 111, 1723–1729.

Selassie, C. D. 2003. History of quantitative structure-activity relationships. *Burger's Medicinal Chemistry and Drug Discovery* (2003) 1-48.

Söderström, G., Sellström, U., De Wit, C. A., Tysklind, M. 2004. Photolytic debromination of decabromodiphenyl ether (BDE 209). *Environ. Sci. Technol.* 38 (2004) 127-132.

Song, R., Duarte, T. L., Almeida, G. M., et al. 2009.Cytotoxicity and gene expression profiling of two hydroxylated polybrominated diphenyl ethers in human H295R adrenocortical carcinoma cells. *Toxicology Letters* 185 (2009) 23-31.

Stanton, D. T., Jurs, P. C. 1990. Development and use of charged partial surface area structural descriptors in computer-assisted quantitative structure-property relationship studies. *Anal. Chem.* 62 (1990) 2323-2329.

Stapleton, H. M., Alaee, M., Letcher, R. J., Baker, J. E. 2004. Debromination of the flame retardant decabromodiphenyl ether by juvenile carp (*Cyprinus carpio*) following dietary exposure. *Environ. Sci. Technol.* 38 (2004) 112-119.

Stapleton, H. M., Dodder, N. G., Offenberg, J. H., Schantz, M. M., Wise, S. A. 2005. Polybrominated diphenyl ethers in house dust and clothes dryer lint. *Environmental Science and Technology* 39:4, 925-931.

Stapleton, H. M., Kelly, S. M., Pei, R., Letcher, R. J., Gunsch, C. 2009. Metabolism of polybrominated diphenyl ethers (PBDEs) by human hepatocytes in vitro. *Environmental Health Perspectives* 117:2 (2009) 197-202.

Suter II, G. W., Barnthouse, L. W., Bartell, S. M., Coemier, S. M., Mackay, D., Mackay, N., Norton, S. B. 2007. Ecological Risk Assessment In: *Organism Level Extrapolation Models*, Glenn W. Suter II, Ed. CRC Press, New York.

Talsness, C. E. 2008.Overview of toxicological aspects of polybrominated diphenyl ethers: A flame-retardant additive in several consumer products. *Environmental Research* 108: 158-167.

Thornberry, N. A. Caspases: Enemies Within. *Science* 281, 1312 (1998).

Tittlemier, S. A., Halldorson, T., Stern, G. A., Tomy, G. T. 2002. Vapor pressures, aqueous solubilities, and henry's law constants of some brominated flame retardants. *Environmental Toxicology and Chemistry* 21:9, 1804-1810.

Todeschini, R., and Consonni, V.2000. *Handbook of Molecular Descriptors*. Weinheim, Germany: Wiley-VCH.

Topliss, J. G., Costello, R. J. 1972. Change correlations in structure-activity studies using multiple regression analysis. *Journal of Medicinal Chemistry* 15:10 (1972) 1066-1068.

Usenko, C. Y., Robinson, E. M., Usenko, S., Brooks, B. W., Bruce., E. D. 2011. PBDE developmental effects on embryonic zebrafish. *Environmental Toxicology and Chemistry* 30:8, 1865-1872.

U.S. Environmental Protection Agency. 2008. Molecular descriptors guide: description of the molecular descriptors appearing in the toxicity estimation software tool.

Viswanadhan, V. N., Ghose, A. K., Revankar, G. R., Robins, R. K. 1990. An estimation of the atomic contribution to octanol-water partition coefficient and molar refractivity from fundamental atomic and structural properties: Its uses in computer aided drug design. *Mathematical and Computer Modeling* 14 (1990) 505-510.

Viswanadhan, V. N., Ghose, A. K., Revankar, G. R., Robins, R. K. 1988. Atomic physicochemical parameters for three dimensional structure directed quantitative structure-activity relationships. 4. Additonal parameters for hydrophobic and dispersive interactions and their application for an automated superposition of certain naturally occurring nucleoside antibiotics. *Journal of Chem. Inf. Comput. Sci* 29, 163-172.

Viswanadhan, V. N., Ghose, A. K., Wendoloski, J. J. 2000. Estimating aqueous salvation and lipophilicity of small organic molecules: A comparative overview of atom/group contribution methods. *Perspectives in Drug Discovery and Design* 19 (2000) 85-98.

Wahl, M., Lahni, B., Guenther, R., Kuch, B., Yang, L., Straehle, U., Strack, S., Weiss, C. 2008. A technical mixture of 2,2',4,4'-tetrabromo diphenyl ether (BDE47) and brominated furans tiggers aryl hydrocarbon receptor (AhR) mediated gene expression and toxicity. *Chemosphere* 73 (2008) 209-215.

Wang, Y., Liu, H., Zhao, C., Liu, H., Cai, Z., Jiang, G. 2005. Quantitative structure-activity relationship models for prediction of the toxicity of polybrominated diphenyl ether congeners. *Environ. Sci. Technol.* 39 (2005) 4961-4966.

Wang, Y., Zhao, C., Ma, W., Liu, H., Wang, T., Jiang, G. 2006. Quantitative structure-activity relationship for prediction of the toxicity of polybrominated diphenyl ether (PBDE) congeners. *Chemosphere* 64 (2006) 515-524.

Wang, H., Joseph, J. A. 1999. Quantifying cellular oxidative stress by dichlorofluorescein assay using microplate reader. *Free Radical Biology & Medicine*, Vol. 27, Nos. 5/6, pp. 612-616.

Wagener, M., van Geerestein, V., 2000. Potential drugs and non-drugs: prediction and identification of important structural features. *Journal of Chem. Inf. Comput. Sci*. 40, 280-292.

Webster, T. F., Harrad, S., Millette, J. R., Holbrook, R. D., Davis, J. M., Stapleton, H. M., Allen, J. G., Mcclean, M. D., Ibarra, C., Abdallah, M. A., Covaci, A. 2009. Identifying transfer mechanisms and sources of deacbromodiphenyl ether (BDE 209) in indoor environments using environmental forensic microscopy. *Environmental Science and Technology* 43:9, 3067-3072.

Wiseman, S. B., Wan, Y., Chang, H., Zhang, X., Hecker, M., Jones, P., Giesy, J.P. 2011. Polybrominated diphenyl ethers and their hydroxylated/methoxylated analogs: Environmental sources, metabolic relationships, and relative toxicities. *Marine Pollution Bulletin* (2011) 1-10.

Yan, C., Huang, D., Zhang, Y. 2010. The involvement of ROS overproduction and mitochondrial dysfunction in PBDE-47-induced apoptosis on Jurkat cells. *Experimental Toxicololgical Pathology*.

Yang, W., Liu, X., Liu, H., Wu, Y., Giesy, J. P., Yu, H. 2009. Molecular docking and comparative molecular similarity indices analysis of estrogenicity of polybrominated diphenyl ethers and their analogues. *Environmental Toxicology* 29 (2009) 1-9.

Ying, X. H., Wei, Z. J., Sen, Y. Q., Hua, W. Y., Ying, Z. J., Xiao, J. H. 2006. QSPR/QSAR models for prediction of the physicochemical properties and biological activity of diphenyl ethers. *Chemosphere* 66 (2007) 1998-2010.

Zhong, H. X., Xu, Y., Cong, H. D., Hui, Y., Xing, Y. F. 2007. Apoptosis induction on human hepatcarcinoma cells Hep G2 of decabrominated diphenyl ether (PBDE-209). *Toxicology Letters* 171 (2007) 19-28.